REPORT No. 901

ANALYSIS OF EFFECT OF BASIC DESIGN VARIABLES ON SUBSONIC AXIAL-FLOW-COMPRESSOR PERFORMANCE

By John T. Sinnette, Jr.

SUMMARY

A blade-element theory for axial-flow compressors has been developed and applied to the analysis of the effects of basic design variables such as Mach number, blade loading, and velocity distribution on compressor performance. A graphical method that is useful for approximate design calculations is presented. The relations among several efficiencies useful in compressor design are derived and discussed. The possible gains in useful operating range obtainable by the use of adjustable stator blades are discussed and a rapid approximate method of calculating blade-angle resettings is shown by an example.

The relative Mach number is shown to be a dominant factor in determining the pressure ratio. Considerable increase in pressure ratio over that for conventional designs can be obtained by producing a velocity distribution that gives relative inlet Mach numbers close to the limiting Mach number on all blade elements. With a given inlet Mach number, the pressure ratio obtainable across a blade row increases and the specific mass flow decreases as the ratio of mean whirl velocity to axial velocity increases for the high-efficiency range of this velocity ratio (that is, near 1).

For compressor designs with a definite Mach number limitation, the velocity distribution in the inlet stage is particularly important because the inlet stage limits both the mass flow and the rotor speed of the compressor and thereby limits the pressure ratio of the later stages as well as the inlet stage. By the use of inlet guide vanes designed to produce a radial variation of axial velocity at the inlet to the first rotor, a substantial increase in stage pressure ratio and a slight increase in specific mass flow over designs based on free vortex with the same turning and Mach number limitations are shown to be possible. In the succeeding stages, the maximum pressure ratio per stage is obtained by increasing the hub diameter to obtain the maximum axial velocity compatible with the Mach number limitation.

INTRODUCTION

The limited amount of research information available for the design of turbojet and turbine-propeller engines has emphasized the need for fundamental research on the compressor as one of the principal components of these power plants. The compressor characteristics that must be considered in the research program are efficiency, size, weight, and operating range or flexibility.

Compressor efficiency has a pronounced effect on the specific fuel consumption of the engine and is therefore especially important for long-range nonstop flights where the fuel weight may amount to several times the useful pay load. Although the efficiency of modern axial-flow compressors is high compared with other types of compressor, substantial gains in engine performance can be derived from further improvement in compressor efficiency.

The importance of size and weight per unit power output of the engine rapidly increases as the flight speed is increased because of the rapid increase in the power required. For some of the high-speed aircraft being developed, consideration of the size and the weight of the power plant becomes of the utmost importance. This analysis is primarily concerned with the compressor size as given by its diameter and length and therefore considers the weight only as it is affected by these variables. The length of a compressor for a given pressure ratio is determined by the pressure ratio per stage and the axial length of a stage; the diameter for a given air flow is determined by the air flow per unit cross-sectional area and by the percentage of the total frontal area utilized. Because of the relatively low pressure ratio per stage, the length of an axial-flow compressor is usually greater than that of a centrifugal compressor, but the over-all diameter is smaller because of the utilization of a larger percentage of the over-all frontal area for air intake. Special effort should therefore be made to reduce the length of an axial-flow compressor with a given over-all pressure ratio by increasing the pressure ratio per stage. Reduction in the diameter for a given air flow by increasing the flow per unit inlet area is also advantageous, particularly for supersonic aircraft, where frontal area is extremely important.

For operation at other than design conditions, the compressor range, or flexibility, becomes important. At engine speeds below the design value, the compressor operating efficiency may be low because of a drop in peak compressor efficiency or because of improper matching of the compressor with the turbine under these conditions. Consequently, the power required to start the engine and the time required to accelerate to design speed may be high. Because of improper matching, compressor surging may be encountered at intermediate speeds, particularly during rapid acceleration. The engine starting and accelerating characteristics with axial-flow compressors are generally poorer than with centrifugal compressors mainly because the efficiency is highest at relatively high compressor speeds and drops appreciably as the

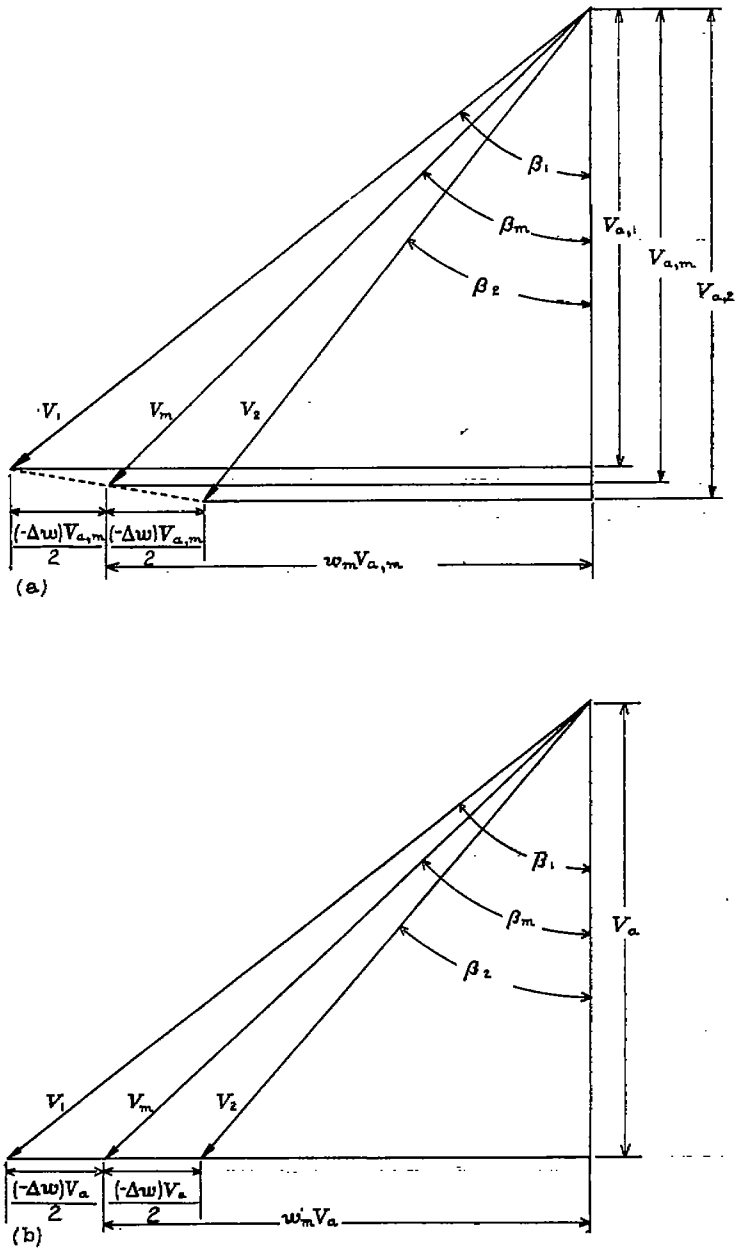

(a) Variable axial velocity. (b) Constant axial velocity.

FIGURE 1.—Relative-velocity diagram for typical blade row.

speed is reduced. The use of high pressure ratios to improve the cycle efficiency accentuates the problems associated with starting and accelerating to design speed and emphasizes the need for the improvement of the range of the compressor.

An analysis was conducted during 1946 at the NACA Cleveland laboratory to determine the effect of basic design variables on subsonic axial-flow-compressor performance. The effect of basic design variables such as Mach number, blade loading, and velocity distribution on efficiency, pressure ratio, and mass flow in axial-flow compressors is analyzed herein in terms of blade-element theory, which is an extension of the theories developed in references 1 and 2. The blade-element analysis neglects the effects of variations in velocity, pressure, and density in the tangential direction at a given axial station between blade rows. On this basis, the relative flow across a blade row is treated as a steady, "one-dimensional," adiabatic, compressible flow, and the velocity ratio, pressure ratio, density ratio, and velocity-of-sound ratio are expressed in terms of the flow-area ratio and the polytropic compression efficiency.

A graphical method that is useful for rapid determination of these ratios for several polytropic compression efficiencies from 0.7 to 1.0 is illustrated. As no restriction is placed on the variation in axial velocity across a blade row, the method and the charts are applicable to a wide variety of compressor-design problems, but a rigorous application requires additional relations based on considerations of radial equilibrium. The charts, however, may be used for rapid approximate design calculations and for the calculation of blade-angle resettings for different operating conditions by considering only mean conditions for the entire annular passage at each axial station.

In order to investigate the effect of the ratio of mean whirl velocity to axial velocity on the efficiency, a blade-element theory of efficiency based on incompressible flow and constant axial velocity is developed. The pressure ratio for constant axial velocity and compressible flow is then expressed in terms of the blade-element drag-lift ratio and the ratio of mean whirl velocity to axial velocity by using the general theory for pressure ratio and by assuming that the polytropic efficiency is equal to the efficiency obtained from the incompressible-flow theory. The effect of the ratio of the mean whirl velocity to axial velocity on the specific mass flow is also derived in terms of compressible-flow theory.

SYMBOLS

The symbols used in this report are defined in alphabetical order. The quantities represented by the symbols df, M, V, w_m, and β depend on the reference frame. When only a single row of blades is being considered, that row of blades is taken as the reference frame. In consideration of a complete stage or any other cases where the reference frame is not clear, it is indicated by the subscript R or S for rotor or stator, respectively.

A	cross-sectional area, square feet
a	velocity of sound, feet per second
C	factor used in expressing total efficiencies in terms of static efficiencies, $\left(\frac{1+\frac{\gamma-1}{2}M_2^2}{1+\frac{\gamma-1}{2}M_1^2}\right)$
C_D	drag coefficient
C_L	lift coefficient
c	blade chord, feet
c_p	specific heat at constant pressure, Btu per pound °F
c_v	specific heat at constant volume, Btu per pound °F
D	blade-profile drag, pounds per foot
F	resultant force on blade element, pounds per foot
f	flow area of entire annular passage taken normal to streamlines at mean radius, square feet
df	flow area taken normal to streamlines between two infinitely close mean stream surfaces, square feet
g	standard acceleration due to gravity, 32.174 feet per second per second
H	total enthalpy per unit mass, foot-pounds per pound

h static enthalpy per unit mass, foot-pounds per pound
J mechanical equivalent of heat, 778 foot-pounds per Btu
K constant in turning-angle relation
L blade-profile lift, pounds per foot
l blade length, feet
M local Mach number, (V/a)
n polytropic exponent for compression
P total pressure, pounds per square foot absolute
p static pressure, pounds per square foot absolute
R gas constant, foot-pounds per pound °R
r radius to blade element, feet
S blade spacing at radius r, feet
T total temperature, °R
t static temperature, °R
U velocity of blade (ωr) at radius r, feet per second
V air velocity with respect to given reference frame, feet per second
W mass flow rate, pounds per second
$W\sqrt{\theta}/(\delta A)$ specific mass flow rate, pounds per second per square foot
w_m ratio of mean whirl velocity to axial velocity (fig. 1)
$-\Delta w$ ratio of decrease in whirl velocity to axial velocity (fig. 1)
α_0 angle of attack of isolated airfoil for zero lift, degrees
β angle between compressor axis and air velocity, or flow angle (fig. 1), degrees
γ ratio of specific heats, (c_p/c_v)
δ ratio of inlet total pressure to standard sea-level pressure (2116.2 lb/sq ft)
ϵ gliding angle, $(\tan^{-1} D/L)$
ζ loss ratio, $(1-\eta_{st,\ t})$
η efficiency of compression
η_{ad} adiabatic efficiency of compression based on static pressure and temperature (unless otherwise specified)
η_p polytropic efficiency of compression based on static pressure and temperature (unless otherwise specified)
θ ratio of inlet total temperature to standard sea-level temperature (518.6 °R)
ρ mass density, slugs per cubic foot
σ blade-element solidity, c/S
ψ angle between blade chord and compressor axis, degrees
ω absolute angular velocity of blade, radians per second

Subscripts:

0 standard sea-level condition (except for α_0)
1 inlet to blade row or stage
2 outlet of blade row
3 outlet of stage
a axial
an annulus
h hub
i incompressible
id ideal
m referred to vector-mean velocity
R rotor reference frame
r radial
S stator reference frame
s secondary
st static
T total
t rotor-blade tip
w whirl
θ tangential

BLADE-ELEMENT THEORY

The blade-element theory is divided into four parts: (1) the general compressible-flow theory in terms of polytropic compression efficiency; (2) the theory of blade-element efficiency in terms of incompressible flow and constant axial velocity; (3) the results of the first two parts combined to obtain the pressure ratio as a function of the drag-lift ratio and the ratio of mean whirl velocity to axial velocity for constant axial velocity; and (4) the specific mass flow in terms of compressible-flow theory.

COMPRESSIBLE-FLOW THEORY

One-dimensional analysis.—Because of the extreme complexity of the actual flow through compressor blades, variout approximate methods of analysis are necessary. Analysis based on one-dimensional flow, that is, flow which is a function of a single coordinate of position, given in various forms and involving various approximations, has proved useful in the analysis of the flow through compressors and turbines and as a basis for design. (See, for example, references 3 to 5.) With an infinite number of blades, a perfect compressible fluid theoretically flows along surfaces of revolution, which constitute flow surfaces, and the velocity, the pressure, and the density are independent of the circumferential position. Because these flow variables may be expressed as a function of a single coordinate of position for the flow between two infinitely close stream surfaces, this flow may be considered as one-dimensional flow. The actual determination of the stream surfaces, of course, constitutes a separate problem involving considerations of radial equilibrium.

The flow of a real fluid through a finite number of blades, however, is dependent on the circumferential position because of the effects of finite blade circulation, viscosity, and turbulence. Also the flow is no longer confined to surfaces of revolution because the circumferential variations in the radial and axial components of velocity generally produce a variation in the inclination of the flow to the compressor axis. A useful one-dimensional approximation to the actual flow may be obtained, however, by using values of velocity, pressure, and density averaged in the circumferential direction and by using for mean stream surfaces, surfaces of revolution through which the average net flow at any axial position is zero.

This one-dimensional analysis is to be used to estimate the change in conditions across a blade row for the flow between two infinitely close mean stream surfaces of revolution. The blade row under consideration is taken as the reference

frame and the flow is steady except for turbulent fluctuations. The pressures, temperatures, densities, and velocity components are the values averaged both with respect to the time and the circumferential position. Because the mean stream surfaces were so chosen that the net flow across them is zero, the mass flow between these surfaces at the inlet to the blade row must be equal to that at the outlet, and the continuity equation may be written

$$\rho_1 V_{a,1} 2\pi r_1 dr_1 = \rho_2 V_{a,2} 2\pi r_2 dr_2$$

where r_1 and $r_1 + dr_1$ are the radial positions ahead of the blade row and r_2 and $r_2 + dr_2$ are the radial positions after the blade row of the mean stream surfaces. The continuity equation may also be expressed in terms of the resultant velocity and the effective flow area:

$$\frac{df_1}{df_2} = \frac{\rho_2 V_2}{\rho_1 V_1} \qquad (1)$$

where the flow area or effective cross-sectional area normal to the relative velocity is given by

$$df = \frac{2\pi r dr}{1 + \frac{V_w^2}{V_a^2} - \frac{V_r^2}{V_a^2}}$$

When $V_r/V_a << 1$ at this station,

$$df \approx \frac{2\pi r dr}{\sqrt{1 + \frac{V_w^2}{V_a^2}}} = 2\pi r dr \cos \beta$$

The one-dimensional approximation to the continuity equation using mean values is exact for incompressible flow and introduces only small errors resulting from the correlation between turbulent fluctuations of velocity and density for compressible flow (reference 6).

The energy equation based on the one-dimensional approximation using mean values can also be employed, but the errors resulting from turbulent fluctuations and from the variation of time-averaged velocity around the circumference may be appreciable if these fluctuations and variations are large, as would be the case near any point of flow separation along the blade surface. The correction for these effects is quite complex (reference 6, equation (43)) and beyond the scope of the present investigation. In the reference frame fixed with respect to the blade row, no work is done by the blades on the air. Some work, however, may be done on the given layer of fluid by adjacent layers of fluid across the boundary surfaces of revolution. The energy exchanges across these surfaces of revolution involve terms similar to those given by equation (43) of reference 6 for the boundary sections at the end stations 1 and 2, but any detailed consideration of these energy exchanges is also beyond the scope of the present investigation. If these energy exchanges are neglected, as well as heat transfer between the blades and the fluid, the energy equation across a rotor-blade row can be written as

$$\frac{V_1^2}{2} - \frac{V_2^2}{2} + \frac{\omega^2 r_2^2}{2} - \frac{\omega^2 r_1^2}{2} = g J c_p t_1 \left(\frac{t_2}{t_1} - 1\right) \qquad (2)$$

The terms involving the angular velocity ω of the reference frame represent the change in potential energy in the centrifugal-force field that results from the rotating reference frame. This equation could, of course, have been obtained by first considering the energy equation for the stationary reference frame and then transforming the results to the rotating reference frame. By the expression of the t_1 outside the parentheses in terms of the velocity of sound

$$a_1 = \sqrt{\gamma g R t_1} = \sqrt{(\gamma - 1) g J c_p t_1} \qquad (3)$$

equation (2) gives, after slight rearrangement,

$$\frac{t_2}{t_1} = 1 + \frac{\gamma - 1}{2} M_1^2 \left[1 - \left(\frac{V_2}{V_1}\right)^2 + \left(\frac{\omega r_2}{V_1}\right)^2 - \left(\frac{\omega r_1}{V_1}\right)^2\right] \qquad (4)$$

The energy equation for the flow through the stator blades differs only in that the reference frame is stationary and therefore $\omega = 0$. The validity of equation (4) is unaffected by frictional losses over the blades. Even separation followed by turbulent mixing would not affect the validity of equation (4) provided that: (1) station 2 is taken far enough downstream that the flow is sufficiently uniform and turbulence has decayed to such an extent that the one-dimensional approximation is adequate, and (2) the energy addition or abstraction from adjacent fluid layers or from the blades by heat conduction is negligible. In case of separation it is generally necessary to go so far downstream to satisfy condition (1) that condition (2) is not even approximately satisfied, but for normal compressor operation without separation both conditions are approximately satisfied at a small distance downstream of the blade row.

Although the temperature ratio t_2/t_1 and the velocity-of-sound ratio a_2/a_1, which is equal to the square root of the temperature ratio, depend only on the variables given in equation (4) independently of frictional losses, the pressure ratio p_2/p_1 and the density ratio ρ_2/ρ_1 depend on an additional variable representing the losses, which can be taken as the polytropic exponent or polytropic efficiency. The relation between the pressure ratio and the density ratio is given by the familiar polytropic relation

$$\frac{p_2}{p_1} = \left(\frac{\rho_2}{\rho_1}\right)^n$$

and, by use of the equation of state for a perfect gas

$$\frac{p}{\rho} = gRt$$

and equation (3), the relations between the various ratios can be concisely written as

$$\frac{p_2}{p_1} = \left(\frac{\rho_2}{\rho_1}\right)^n = \left(\frac{t_2}{t_1}\right)^{\frac{n}{n-1}} = \left(\frac{a_2}{a_1}\right)^{\frac{2n}{n-1}} \qquad (5)$$

The value of n depends on the losses and can be expressed in terms of the polytropic compression efficiency, as discussed in the following section.

The density ratio can be eliminated from equation (1) by means of equations (4) and (5) to obtain the flow-area ratio as an explicit function of the velocity ratios, the inlet Mach number, and the polytropic exponent:

$$\frac{df_1}{df_2}=\frac{V_2}{V_1}\left\{1+\frac{\gamma-1}{2}M_1^2\left[1-\left(\frac{V_2}{V_1}\right)^2+\left(\frac{\omega r_2}{V_1}\right)^2-\left(\frac{\omega r_1}{V_1}\right)^2\right]\right\}^{\frac{1}{n-1}} \tag{6}$$

For axial-flow compressors, radial flow can usually be neglected; consequently r_1 equals r_2 and equation (6) becomes

$$\frac{df_1}{df_2}=\frac{V_2}{V_1}\left\{1+\frac{\gamma-1}{2}M_1^2\left[1-\left(\frac{V_2}{V_1}\right)^2\right]\right\}^{\frac{1}{n-1}} \tag{6a}$$

which does not contain ω and hence has the same form for rotating and stationary blades. The validity of equations (2), (4), (6), and (6a) depends on the use of the given blade row as reference frame for the velocities, the flow areas, and the Mach number.

General efficiency relations.—The expression of the exponent in terms of an efficiency is desirable. The polytropic efficiency based on static pressures and temperatures is closely related to the polytropic exponent and serves as a convenient and useful measure of performance. The significance of this efficiency and its relation to other efficiencies frequently used and to the polytropic exponent requires consideration. Different expressions for the polytropic efficiency are obtained for compression and expansion processes because the terms representing input and output are interchanged. Only compression efficiency is considered here. The following analysis assumes that the actual process is adiabatic; that is, no heat transfer is involved.

Compressor efficiency is usually defined as the ratio of the ideal work of compression from the initial to the final total pressure to the actual work done by the rotor blades on the air. This efficiency is satisfactory for over-all compressor-performance representation, but gives no information on the efficiency with which static pressure is increased and is meaningless when applied to stationary elements of the compressor (stator blades and outlet diffuser) as no work is done by these elements (in terms of the usual stationary reference frame). In general, the work input by a given element of the compressor depends on the reference frame. For the reference frame fixed with respect to a given blade row, as used in the blade-element analysis, the work input by the given blade row is zero regardless of whether these blades are rotor blades or stator blades. The total mechanical energy available for increasing the pressure in the given process must therefore be considered.

For an adiabatic process considered herein, the available energy is equal to the change in (static) enthalpy Δh in the process (which is obviously independent of the reference frame). The ideal energy in foot-pounds per pound required for compression between the same initial and final pressures in a continuous-flow process is given by

$$\frac{1}{g}\int_{p_1}^{p_2}\frac{dp}{\rho_{id}(p)}$$

where $\rho_{id}(p)$ is the mass density as a function of pressure for the ideal process. The subscripts 1 and 2 used here and in other general equations defining the efficiencies or showing their interrelations indicate the initial and final states for any portion of the compression process considered and are not necessarily limited to the inlet and the outlet of a blade row as for most of the equations in the blade-element theory. The general definition of static compression efficiency, that is, the efficiency with which mechanical energy is utilized to increase the static pressure, is equal to the ratio of ideal energy to the actual energy required for the compression, and is therefore

$$\eta_{st}=\frac{\frac{1}{g}\int_{p_1}^{p_2}\frac{dp}{\rho_{id}(p)}}{\Delta h} \tag{7}$$

and differs from the corresponding efficiency based on total pressure only in the replacement of enthalpies and pressures based on total (stagnation) conditions by those based on static conditions. Unlike the efficiency based on total conditions, the efficiency based on static conditions is independent of the reference frame and can be applied equally well to stationary and rotating components of the compressor. For these reasons, an efficiency based on static conditions is introduced.

The efficiency is incompletely specified, however, until the ideal process of compression is given. The only ideal processes that will be considered here are the adiabatic and polytropic processes that form the basis for the corresponding adiabatic and polytropic efficiencies. The ideal adiabatic process is a reversible adiabatic process between the same initial pressures and temperatures and the same final pressure as the actual process. (The final temperatures will be different unless the efficiency is 1.) The ideal polytropic process is a reversible polytropic process with a constant exponent and with the same initial and final pressures and temperatures as the actual process. Thus the ideal adiabatic process differs from the actual process in the final temperature, whereas the ideal polytropic process differs from the actual process in the existence of heat addition to the gas for the ideal process.

For compression without heat transfer, the relation between adiabatic and polytropic efficiency is shown in appendix A to be given by

$$\eta_{ad}=\frac{\left(\frac{p_2}{p_1}\right)^{\frac{\gamma-1}{\gamma}}-1}{\left(\frac{p_2}{p_1}\right)^{\frac{\gamma-1}{\gamma\eta_p}}-1} \tag{8}$$

for efficiencies and pressure ratio based on either total or static conditions. When the pressure ratio is plotted on a logarithmic scale (fig. 2), a nearly straight-line relation is

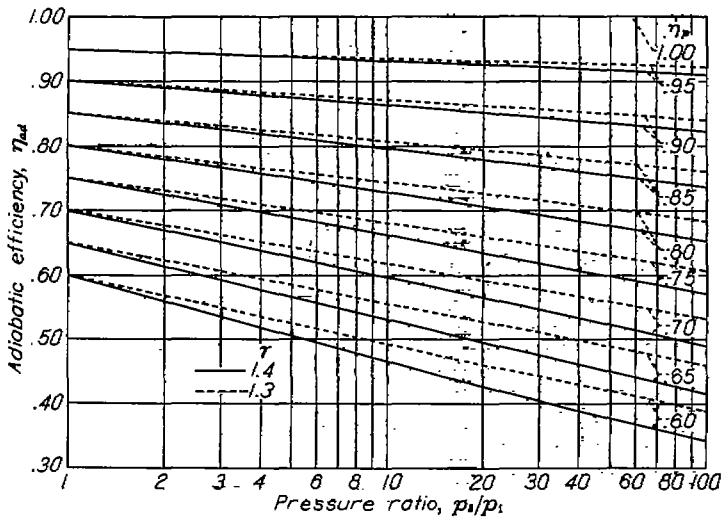

FIGURE 2.—Variation of adiabatic efficiency η_{ad} with pressure ratio for polytropic efficiencies η_p from 0.60 to 1.00 and specific-heat ratios γ of 1.3 and 1.4 for adiabatic compression.

obtained with the two efficiencies equal at a pressure ratio of 1. For the pressure ratios (generally less than 1.2) obtained across a row of blades of subsonic designs, the difference between adiabatic and polytropic efficiencies is negligible (fig. 2). The polytropic exponent for compression is shown in appendix A to be given in terms of the polytropic efficiency by the relation

$$n=\frac{\eta_p}{\eta_p-\frac{\gamma-1}{\gamma}} \qquad (9)$$

The relation between the adiabatic and polytropic efficiencies based on total and static conditions is also shown in appendix A to be given by

$$\eta_{ad,T}=\eta_{ad,st}\frac{\left(\frac{P_2}{P_1}\right)^{\frac{\gamma-1}{\gamma}}-1}{\left(\frac{P_2}{P_1}\right)^{\frac{\gamma-1}{\gamma}}-1+(1-C)(1-\eta_{ad,st})}$$

and

$$\eta_{p,T}=\eta_{p,st}\frac{\log\left(\frac{P_2}{P_1}\right)^{\frac{\gamma-1}{\gamma}}}{\log\left(\frac{P_2}{P_1}\right)^{\frac{\gamma-1}{\gamma}}-(1-\eta_{p,st})\log C}$$

where

$$C=\frac{1+\frac{\gamma-1}{2}M_2^2}{1+\frac{\gamma-1}{2}M_1^2}$$

From these equations, for both the adiabatic efficiency and the polytropic efficiency no difference exists in the corresponding efficiencies based on total and static conditions when the static efficiency is equal to 1 or when $C=1$, that is, when $M_1=M_2$. In general, the difference between the total and static efficiencies (for both adiabatic and polytropic efficiencies) decreases as the pressure ratio or efficiency increases or as C approaches 1. For over-all performance representation of a compressor under normal operating conditions, the difference between the total and static efficiencies is generally small. For example, for $P_2/P_1=5$, $M_1=0$, $M_2=0.5$, and $\eta_{ad,st}=0.80$, the total efficiency is 0.814. If the Mach numbers at the inlet and outlet measuring stations are nearly equal, the difference in efficiencies will be considerably less.

The discussion on efficiency may be summarized: The difference between the adiabatic and polytropic efficiencies is usually negligible for the pressure ratios obtainable across a blade row or a stage but becomes important when the over-all efficiency of a compressor is considered. The chart relating the two efficiencies (fig. 2) is useful in estimating the over-all adiabatic efficiency of a compressor for adiabatic compression in terms of an average stage efficiency represented by the polytropic efficiency. Efficiencies based on static-pressure and static-temperature changes are required in considering the compression across individual blade rows and the same basis for efficiency can be used for over-all compressor-performance representation. If the conventional adiabatic efficiency for the over-all performance in terms of total pressures and temperatures is desired, a small correction may be applied to the adiabatic efficiency based on static states to take account of the change in Mach number across the compressor.

Graphical representation in terms of polytropic efficiency.—A graphical representation of equation (6a) in terms of η_p (equation (9)) is useful for the rapid determination of any one of the variables in terms of the others (fig. 3). By use of equations (4) (with $r_1=r_2$), (5), and (9), the velocity-of-sound ratio a_2/a_1, temperature ratio t_2/t_1, density ratio ρ_2/ρ_1, and pressure ratio p_2/p_1 may also be explicitly expressed in terms of the same variables as were used for the flow-area ratio. For the applications considered, however, the replacement of the velocity ratio by the flow-area ratio as one of the independent variables by the use of the implicit equation (6a) is convenient. The graphical representation of these ratios with the inlet Mach number, flow-area ratio, and polytropic efficiency as independent variables is shown in figure 4. Figures 3 and 4 show that the polytropic efficiency has a rather large effect on some of the flow relations especially at Mach numbers approaching 1. Appreciable error in the flow relations for a given type of blading may therefore result if the calculations are based on isentropic flow.

Charts similar to figures 3 and 4 may be used for a wide variety of design calculations, but a rigorous application requires additional relations based on considerations of radial equilibrium and will not be further developed here. The charts, however, may be used for rapid approximate design calculations and for the calculation of blade-angle rosettings for different operating conditions by considering only mean conditions for the entire annular passage. An example of this type of application is given in appendix B.

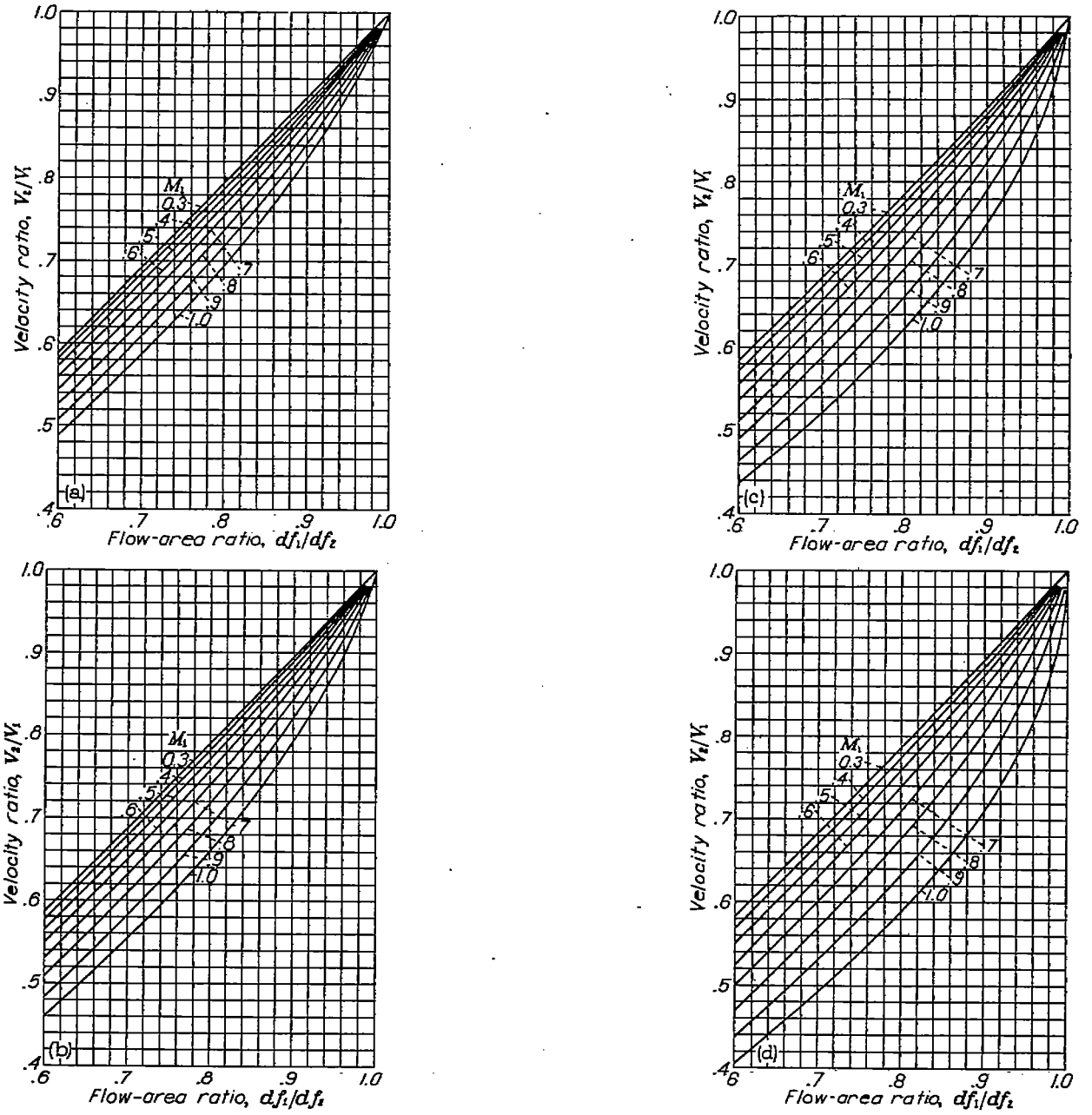

(a) Polytropic efficiency η_p, 0.7.
(b) Polytropic efficiency η_p, 0.8.
(c) Polytropic efficiency η_p, 0.9.
(d) Polytropic efficiency η_p, 1.0.

FIGURE 3.—Velocity ratio V_2/V_1 for steady, one-dimensional flow as function of flow-area ratio df_1/df_2, inlet Mach number M_1, and polytropic efficiency η_p for adiabatic compression with specific-heat ratio γ of 1.4.

BLADE-ELEMENT EFFICIENCY

The exact analysis of the efficiency of an axial-flow compressor is extremely complex and must be based on a detailed knowledge of the flow processes involved, but an approximate analysis may be made by treating the flow and the corresponding losses near the ends of the blades separately from those for the central portion of the annular passage. The losses near the ends of the blades will be discussed under the section Application of Blade-Element Theory to Compressor Design. The following analysis of blade-element efficiency applies to the main portion of the flow and is based on the assumptions of incompressible flow, constant axial

velocity across the blade row (fig. 1 (b)), and no radial flow. The usual magnitudes of radial flow, variations in axial velocity, and compressibility effects encountered in subsonic-compressor designs are assumed to have little effect on the blade-element efficiency. The theory is similar to that presented in reference 2, but the efficiency based on static-pressure rise for a single blade row treated as a diffuser is used instead of the stage efficiency based on power input.

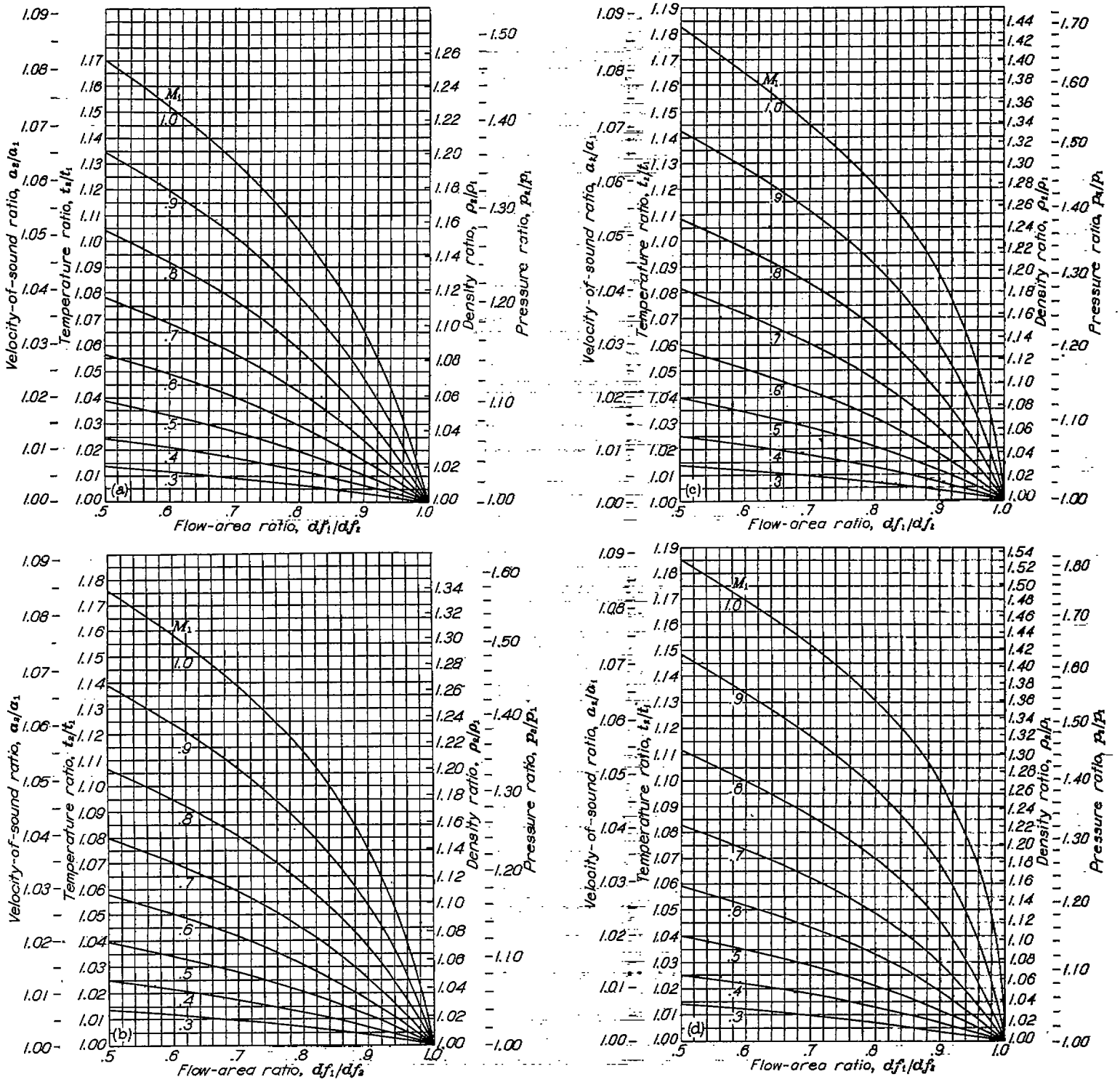

(a) Polytropic efficiency η_p, 0.7.
(b) Polytropic efficiency η_p, 0.8.
(c) Polytropic efficiency η_p, 0.9.
(d) Polytropic efficiency η_p, 1.0.

FIGURE 4.—Velocity-of-sound ratio a_2/a_1, temperature ratio t_2/t_1, density ratio ρ_2/ρ_1, and pressure ratio p_2/p_1 for steady, one-dimensional flow as functions of flow-area ratio df_1/df_2, inlet Mach number M_1, and polytropic efficiency η_p for adiabatic compression with specific-heat ratio γ of 1.4.

The blade-element efficiency for a blade row is shown in appendix A to be given by

$$\eta_{bl,t}=\frac{1-\frac{1}{w_m}\frac{D}{L}}{1+w_m(D/L)} \tag{10}$$

or

$$\eta_{bl,t}=\frac{\tan(90°-\beta_m)}{\tan(90°-\beta_m+\epsilon)} \tag{11}$$

which, as might be expected, is the same as the profile efficiency of a propeller.

The variation of the blade-element efficiency with ratio of the mean whirl velocity to axial velocity w_m is shown in figure 5 for values of D/L of 0, 0.05, and 0.10. For optimum angles of attack and efficient blading, the value of D/L should be less than 0.05 and high blade-element efficiencies should therefore be obtained. Because of the large variations in axial velocity, the large and complex secondary flow, and the frictional effects of the walls, the blade-element analysis cannot be expected to give an accurate representation for the efficiency in the region of the blade root and the blade tip.

Because the analysis applies to either rotor or stator blades, the optimum value of w_m is the same for each and the resulting optimum velocity diagram for the stage is symmetrical. For a symmetrical velocity diagram, the losses and the ideal pressure rises are the same for the rotor and stator blades (if differences in the boundary-layer conditions are assumed not to affect the value of D/L) and the efficiency of conversion to static pressure for the stage is the same as for each blade row. Consequently, figure 5 also represents the stage efficiency for a symmetrical diagram. The efficiency for a symmetrical velocity diagram obtained from figure 5 differs slightly from that obtained by use of figure 17 of reference 2 because the figure of reference 2 is based on a linear approximation to the exact equation (10), namely

$$\eta_{st,t}=1-\zeta\approx 1-\frac{D}{L}\left(\frac{1}{w_m}+w_m\right)$$

For a nonsymmetrical velocity diagram, the blade-element efficiency for the stage is the weighted average of the blade-element efficiencies for the rotor and stator blades with the weighting factors given by the ideal pressure rise of each. The relations derived in the present analysis should be accurate over a wide range of values of D/L and w_m. Because the curves of figure 5 are fairly flat in the region of peak efficiency, a moderate deviation from the optimum value of w_m produces only a small loss in blade-element efficiency.

BLADE-ELEMENT PRESSURE RATIO

General considerations.—If radial flow is neglected, the pressure ratio across a row of blades, either rotor or stator, is given by

$$\frac{p_2}{p_1}=\left\{1+\frac{\gamma-1}{2}M_1^2\left[1-\left(\frac{V_2}{V_1}\right)^2\right]\right\}^{\frac{\gamma\eta_p}{\gamma-1}} \tag{12}$$

which is obtained from equations (4), (5), and (9). For a given value of γ, the pressure ratio thus depends only on the inlet Mach number M_1, the velocity ratio V_2/V_1, and the polytropic efficiency η_p. If the efficiency could be held constant, very high pressure ratios obviously could be obtained by increasing the Mach number. With conventional compressor designs, however, the efficiency has been found to drop very rapidly if the inlet Mach number is increased much beyond the critical Mach number of the blades. For this reason, designs for inlet Mach numbers appreciably above the critical Mach number of the blades have generally been considered impractical. The high efficiencies that have been obtained with supersonic diffusers, however, strongly suggest that compressors of high efficiency and pressure ratio are possible with supersonic velocities entering the blades, but any detailed consideration of such compressors is beyond the scope of the present investigation.

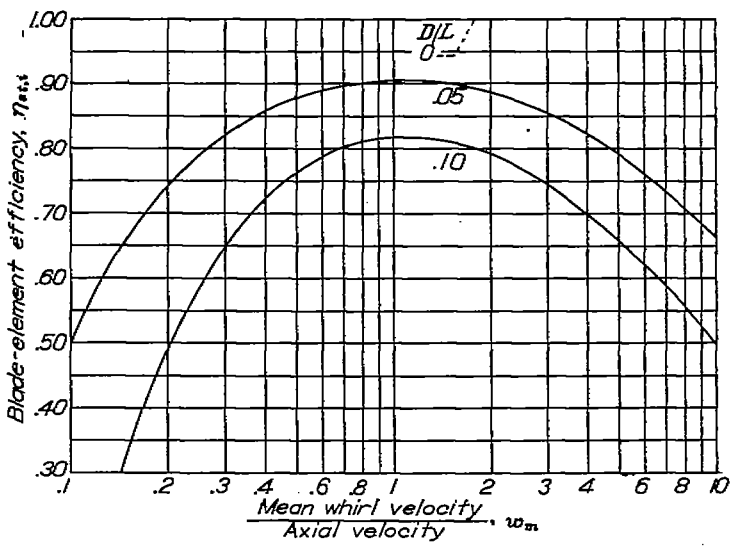

FIGURE 5.—Efficiency of blade element $\eta_{bl,t}$ as function of ratio of mean whirl velocity to axial velocity w_m and of drag-lift ratio D/L.

With given Mach number and polytropic efficiency, equation (12) shows that the pressure ratio increases as the velocity ratio V_2/V_1 decreases, but at a continuously decreasing rate, and reaches a maximum at a velocity ratio of 0. Not all the static-pressure rise resulting from a decrease in the relative velocity, however, represents a gain in the total-pressure ratio of the compressor. Only changes in the whirl component of velocity (for $r_1=r_2$) are effective in increasing the total enthalpy and hence the total pressure, as is evident from Euler's equation,

$$\Delta H=\frac{1}{g}(V_{2,w,s}-V_{1,w,s})U$$

for $r_1=r_2$. (See reference 7 for a detailed discussion of the applications of Euler's equation.) Although the total pressure is increased only across the rotor blades, the stator blades generally must change the whirl component of velocity by about the same amount in the opposite direction in order that the process can be repeated in the next stage. Changes in the axial component of velocity have no direct effect on the total-pressure ratio obtained.

The possibility of an indirect effect of change in axial velocity on the total-pressure ratio must, however, be considered. Schicht proposed increasing the total-pressure ratio by using a rapidly increasing axial component of velocity

through the rotor (reference 3). The argument for this procedure is that, when the usual adverse pressure gradient, which tends to produce flow separation, is reduced by increasing the axial velocity, a larger change in whirl velocity and hence a greater total-pressure ratio can be obtained. This method may be effective for single-stage, low-speed blowers in applications where high discharge velocity is desired. The method is unsuitable, however, for high-speed, multistage axial-flow compressors, because, in order to be able to repeat the process in a number of stages, the axial velocity has to be again reduced through the stator blades. The argument that an increasing axial velocity makes possible a large change in whirl velocity in the rotor blades also indicates that obtaining the same change in whirl velocity with reasonable efficiency in the stators, where the axial velocity is decreasing, would be very difficult. Excessively high Mach numbers at the inlet to the stators are also encountered if reasonable rotor speeds and inlet Mach numbers to the rotor blades are used.

Thus, for subsonic-compressor designs with definite Mach number limitations, little if anything appears to be gained in increased over-all pressure ratio by appreciable changes in axial velocity across any blade row. A gradual change in the axial velocity through a multistage compressor may be desirable to obtain favorable conditions at the inlet to each stage, but any increase in over-all total-pressure ratio that is obtained results principally from realizing the optimum Mach number at the inlet to each stage rather than from the direct effect of change in axial velocity within the stage on the total-pressure ratio across the stage.

In analyzing the blade-element performance of a single stage in relation to its effect on the total-pressure ratio of the compressor, the actual stage can therefore be considered replaced by an equivalent stage with the same inlet Mach number and changes in whirl velocity but with constant axial velocity. Because the static-pressure ratio across such an equivalent stage is practically the same as the total-pressure ratio, the consideration of static-pressure ratios alone across the equivalent stage is sufficient in evaluating the performance of stages designed to give maximum total-pressure ratio in a given number of stages.

Pressure ratio based on constant axial velocity.—For constant axial velocity, the velocity ratio across a blade row is given by

$$\frac{V_2}{V_1}=\frac{\cos\beta_1}{\cos\beta_2}$$

and hence from equation (12) the pressure ratio is

$$\frac{p_2}{p_1}=\left\{1+\frac{\gamma-1}{2}M_1^2\left[1-\left(\frac{\cos\beta_1}{\cos\beta_2}\right)^2\right]\right\}^{\frac{\gamma\eta_p}{\gamma-1}} \qquad (13)$$

The minimum possible value of the velocity ratio for a given inlet-air angle β_1 is equal to the cosine of the inlet-air angle. For constant axial velocity across the blade row, the inlet-air angle must thus be large to obtain appreciable diffusion through any row of blades.

The actual pressure ratio that can be obtained, however, depends also on the practical limitations on the turning of the air. The maximum amount of turning that is practical without flow separation and appreciable loss of efficiency varies appreciably with the value of w_m. Several different parameters have been used to represent this limitation. A natural extension of the idea of blade loading for isolated airfoils is the limitation based on $C_L\sigma$ (references 2, 8 (p. 39), and 9), which is a measure of the loading on a row of blades rather than on the individual blades. Another limitation based on the maximum allowable value of $-\Delta w$, which remains nearly constant over a fairly large range of values of w_m, will also be considered. For brevity both of these limitations will be designated blade-loading limitations.

The relation between lift coefficient, solidity, and whirl-velocity ratios is obtained from reference 2, equation (21), as

$$C_L\sigma=\frac{2(-\Delta w)}{\sqrt{w_m^2+1}\,[1+(D/L)w_m]} \qquad (14)$$

or expressed in terms of angles by use of figure 1 (b) as

$$C_L\sigma=\frac{2\cos\beta_m(\tan\beta_1-\tan\beta_2)}{1+(D/L)\tan\beta_m}$$

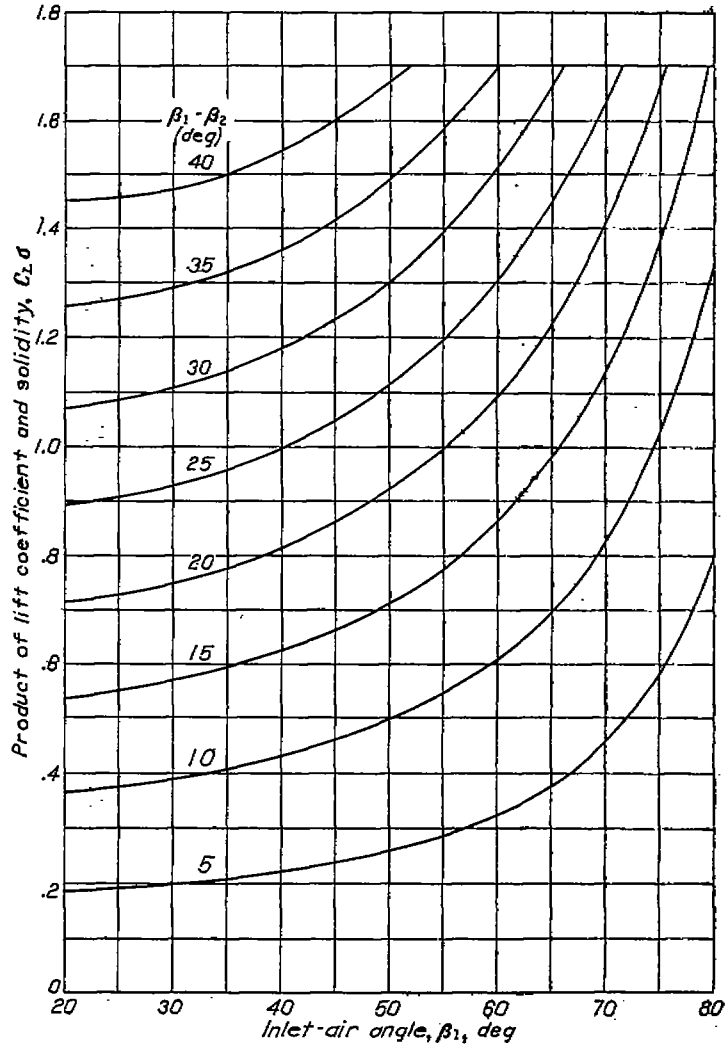

FIGURE 6.—Relation between product of lift coefficient and solidity $C_L\sigma$, inlet-air angle β_1, and turning angle $\beta_1-\beta_2$ for drag-lift ratio D/L of 0.

A graphical representation based on these relations showing $C_L\sigma$ as a function of inlet-air angle and turning angle for D/L equal to 0 is shown in figure 6. For most practical applications the term $(D/L)\tan\beta_m$ can be neglected, but if high accuracy is desired the effect of drag can be taken into account by dividing the value of $C_L\sigma$ obtained from figure 6 by $1+(D/L)\tan\beta_m$. The pressure ratio, expressed

in terms of the ratio w_m of mean whirl velocity to axial velocity, is given, as shown in appendix A, by

$$\frac{p_2}{p_1}=\left\{1+(\gamma-1)M_1^2\frac{w_m(-\Delta w)}{1+\left[w_m+\frac{(-\Delta w)}{2}\right]^2}\right\}^{\frac{\gamma\eta_p}{\gamma-1}} \tag{15}$$

The value of $-\Delta w$ in terms of $C_L\sigma$ is obtained by solving equation (14) for $-\Delta w$.

$$-\Delta w=\frac{1}{2}C_L\sigma\sqrt{1+w_m^2}\left(1+w_m\frac{D}{L}\right) \tag{16}$$

The pressure ratio as a function of w_m for $M_1=0.7$ and $C_L\sigma=1.0$ for three values of D/L is shown in figure 7 (a). The polytropic efficiency was assumed equal to the efficiency for incompressible flow given by equation (10). For the isentropic case ($D/L=0$), the pressure ratio increases asymptotically to a maximum as w_m increases but is very near the maximum value at $w_m=4$. As the value of D/L is increased, the maximum pressure ratio is obtained at progressively lower values of w_m because of the drop in efficiency when w_m is increased beyond 1 (fig. 5). Even with a value of D/L of 0.10, the maximum pressure ratio occurs at a value of w_m more than twice that for maximum efficiency. The effect of $C_L\sigma$ on the pressure ratio is shown in figure 7 (b). A point of diminishing returns is rapidly approached as $C_L\sigma$ is increased. The corresponding decreasing rate of increase in total-pressure ratio of a stage is associated with the decrease in rotor speed resulting if a constant relative inlet Mach number is to be maintained as $-\Delta w$ is increased.

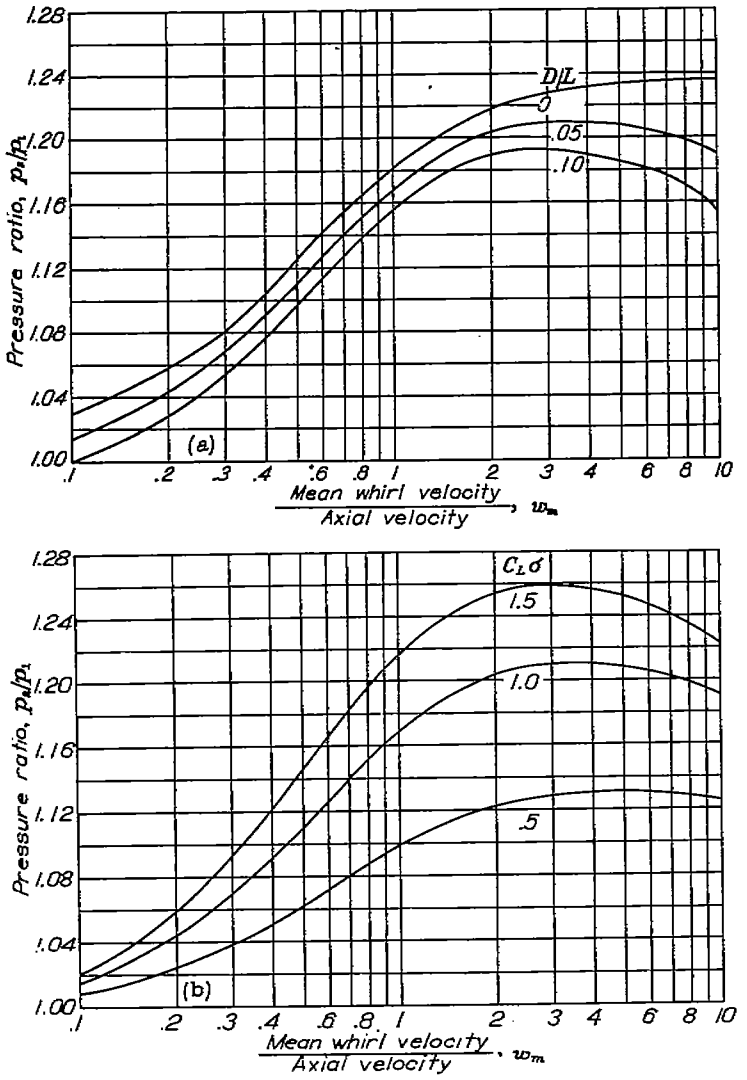

(a) Product of lift coefficient and solidity $C_L\sigma$, 1.0
(b) Drag-lift ratio D/L, 0.05.

FIGURE 7.—Pressure ratio across blade row p_2/p_1 as function of ratio of mean whirl velocity to axial velocity w_m for inlet Mach number M_1 of 0.7.

The variation in pressure ratio with w_m shown in figure 7 is quite different from the familiar variation (references 8 (pp. 99-105) and 10) when the rotor speed instead of the relative inlet Mach number is constant. The variation in pressure ratio with w_m for a symmetrical velocity diagram when the rotor-blade-element Mach number U/a_1 is constant is shown in figure 8 with the inlet relative Mach number M_1

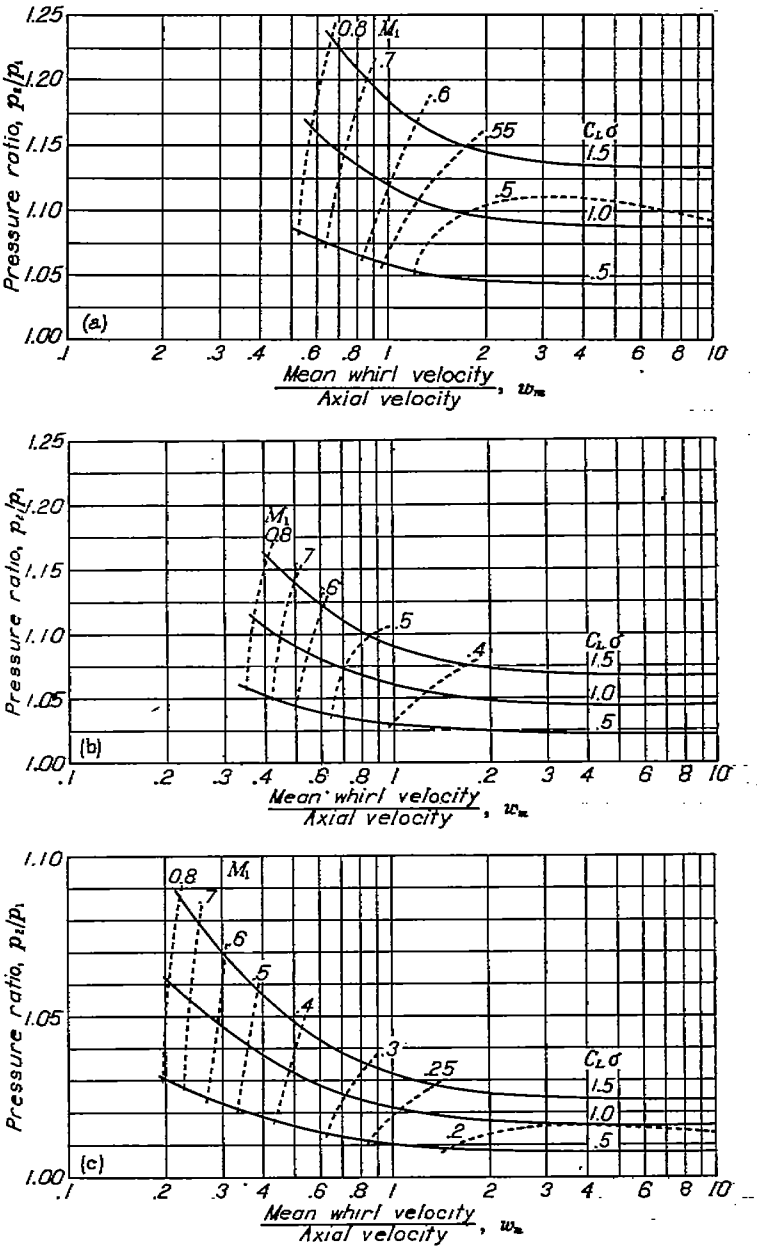

(a) Rotor-blade-element Mach number U/a_1, 0.7.
(b) Rotor-blade-element Mach number U/a_1, 0.5.
(c) Rotor-blade-element Mach number U/a_1, 0.3.

FIGURE 8.—Pressure ratio p_2/p_1 across blade row as function of ratio of mean whirl velocity to axial velocity w_m and product of lift coefficient and solidity $C_L\sigma$ for constant rotor-blade-element Mach number U/a_1, symmetrical velocity diagram, and drag-lift ratio D/L of 0.05. Values of inlet Mach number M_1 shown as contours.

shown as contours. These curves are based on the relation

$$\frac{p_2}{p_1}=\left[1+\frac{\gamma-1}{4}\left(\frac{U_1}{a_1}\right)^2\frac{(-\Delta w)}{w_m}\right]^{\frac{\gamma\eta_p}{\gamma-1}}$$

which is obtained by substituting the relation for a symmetrical velocity diagram (fig. 9)

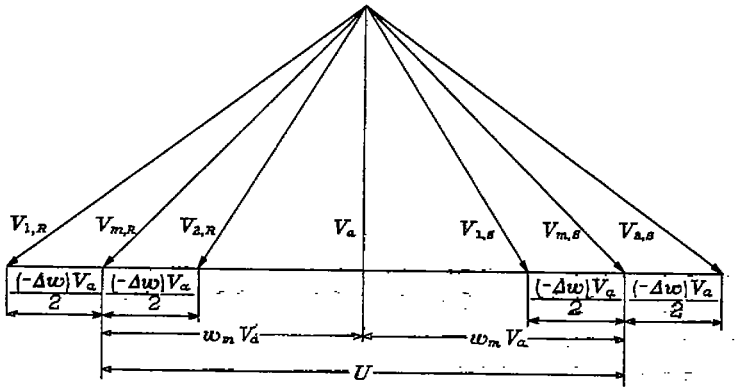

FIGURE 9.—Symmetrical velocity diagram for rotor blades showing velocities relative to rotor and stator reference frames.

$$M_1=\frac{\sqrt{1+\left[w_m+\frac{(-\Delta w)}{2}\right]^2}}{2w_m}\frac{U}{a_1}$$

in equation (15). The pressure ratio given in figure 8 actually represents that across the first row of blades of a symmetrical stage. If the axial velocity is maintained constant, as is assumed here, the pressure ratio across the second row of blades will be slightly less than that across the first row because of the higher velocity of sound and hence lower relative Mach number at the inlet to the second row of blades of the stage.

The increase in pressure ratio with decreasing w_m is due to the increase in relative Mach number as the value of w_m is decreased (fig. 8). The curves have been extended only up to a relative Mach number of about 0.8 because the assumption of constant D/L cannot be expected to hold above that Mach number. The shape of the curves is essentially the same for the three different rotor speeds shown in figure 8, but the actual pressure ratios at the same value of w_m are, of course, different because of the different Mach number. Moreover, the curves are extended to lower values of w_m at the lower rotor speeds (figs. 8 (b) and 8 (c)) because of the shift of the limiting Mach number contour of 0.8 to the left. The important conclusion to be drawn from figure 8 is that, for a given rotor speed, the pressure ratio can be raised by increasing the design axial velocity up to the point where the effect of additional blade drag resulting from compression shock, corresponding to an increase in D/L, counterbalances the direct effect of higher Mach number.

Although limitations on blade loading based on $C_L\sigma$ are widely used in fan and compressor design, it is not always realized that the maximum allowable value of $C_L\sigma$ varies with the value of w_m and hence with the blade stagger. Unfortunately, only meager experimental data on this important point are available. According to Howell in a British report, the allowable value of C_L drops appreciably with increasing values of w_m, and a constant $-\Delta w$ (equal to $\tan\alpha_1-\tan\alpha_2$ in Howell's notation) is a better limitation at values of w_m less than 1.

The pressure ratio is shown in figure 10 for a constant

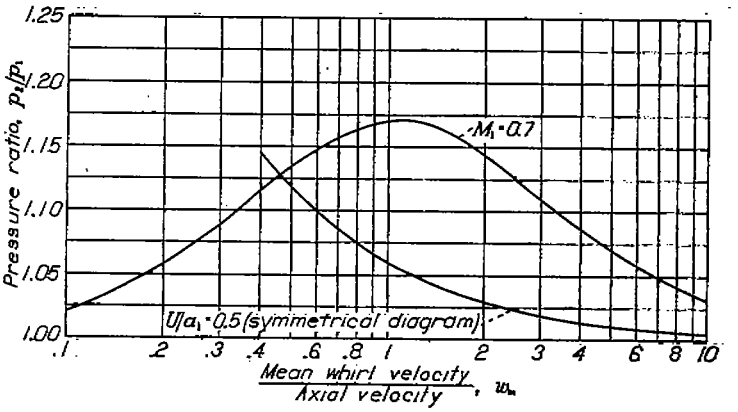

FIGURE 10.—Pressure ratio across blade row as function of ratio of mean whirl velocity to axial velocity w_m with ratio of decrease in whirl velocity to axial velocity $-\Delta w$ of 0.742 and drag-lift ratio D/L of 0.05.

value of $-\Delta w=0.742$ (corresponding to its value for $C_L\sigma=1$, $w_m=1$, and $D/L=0.05$), for a constant value of M_1, and for a constant value of U/a_1. The available data seem to indicate that, when the value of w_m is less than 1, the limitation based on a constant $-\Delta w$ is preferable; whereas, at values of w_m greater than 1, the limitation based on a constant $C_L\sigma$ is better. On the basis of either of these limitations on the turning of the air, for a given inlet Mach number a considerable drop in pressure ratio occurs if w_m is decreased much beyond 1.

For a constant value of w_m and a given blade-loading limitation, equation (15) shows that the pressure ratio increases with increasing Mach number within the range of Mach numbers over which the efficiency change is inappreciable. The pressure ratio also increases with increasing Mach number when the rotor speed is held constant (fig. 8). The Mach number thus plays a dominant role in determining the pressure ratio. In order to obtain high pressure ratios per stage on all stages, a compressor should therefore be designed for a velocity distribution that gives as nearly as possible the limiting relative Mach number at the inlet to all blade elements.

SPECIFIC MASS FLOW

The mass flow through a unit cross-sectional area of a compressor is given by

$$\frac{W}{A}=g\rho_T a_T\frac{M_S\cos\beta_S}{\left(1+\frac{\gamma-1}{2}M_S^2\right)^{\frac{\gamma+1}{2(\gamma-1)}}} \qquad (17)$$

where the quantities M_S and β_S are with respect to a stationary reference frame. (See appendix A.) Because both ρ_T and a_T increase through the compressor, the mass flow per unit area for a given absolute Mach number M_S and flow angle β_S also increases through the compressor. Only at the

compressor inlet does the mass flow per unit area therefore provide an essential limitation on the total mass flow for a compressor of a given diameter. The mass flow per unit cross-sectional area corrected to standard sea-level conditions is referred to hereinafter as "specific mass flow." The specific mass flow for dry air with γ equal to 1.4 is given by (appendix A)

$$\frac{W\sqrt{\theta}}{\delta A}=\frac{85.4M_S\cos\beta_S}{(1+0.2M_S^2)^3} \tag{18}$$

The maximum specific mass flow is obtained when $\beta=0$ and $M_S=1$ and is equal to 49.4 pounds per second per square foot. For this condition to occur ahead of the first rotor, the inlet Mach number relative to the first rotor must be supersonic. The decrease in specific mass flow for a moderate change in M_S or β_S from the optimum values, however, is slight. For example, for a value of M_S of 0.7, the reduction in specific mass flow is only 9 percent.

For a subsonic-compressor design with a given Mach number limitation and rotor speed, the maximum specific mass flow is obtained with an approximately symmetrical velocity diagram, because any appreciable deviation from symmetry requires a substantial reduction in the allowable axial velocity to keep within the Mach number limitation on both the rotor and stator blades. For a symmetrical velocity diagram and a relative inlet Mach number $M_{1,R}$ the specific mass flow is given (appendix A) by

$$\frac{W\sqrt{\theta}}{\delta A}=\frac{85.4M_{1,R}}{\left\{1+0.2M_{1,R}^2\dfrac{1+\left[w_m-\dfrac{(-\Delta w)}{2}\right]^2}{1+\left[w_m+\dfrac{(-\Delta w)}{2}\right]^2}\right\}^3\sqrt{1+\left[w_m+\dfrac{(-\Delta w)}{2}\right]^2}} \tag{19}$$

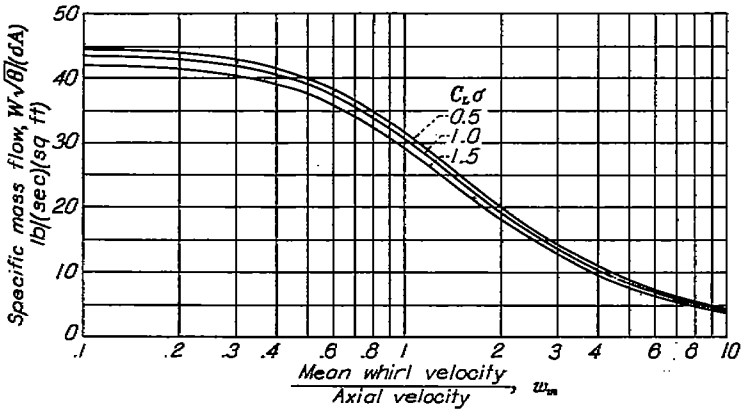

FIGURE 11.—Specific mass flow as function of ratio of mean whirl velocity to axial velocity w_m for inlet Mach number M_1 of 0.7 and symmetrical velocity diagram.

The variation of the specific mass flow w_m is shown in figure 11 for a symmetrical velocity diagram with given Mach number and $C_L\sigma$ limitations. The maximum specific mass flow is obtained at low values of w_m but the rate of increase becomes very small as w_m is decreased below 0.4. At a value of w_m equal to 1, corresponding to the maximum blade-element efficiency, the specific mass flow is about 70 percent of its maximum value.

APPLICATION OF BLADE-ELEMENT THEORY TO COMPRESSOR DESIGN

EFFICIENCY

The blade-element theory alone does not account for all the aerodynamic losses in a compressor. The friction of the annular walls and the large secondary flows near the ends of the blades introduce additional losses. No adequate theoretical analysis of these losses is at present available, but a semiempirical analysis has been given by Howell (reference 11), which appears to approximate closely the over-all compressor efficiency over a range of operation. The losses are expressed in terms of an effective drag coefficient at the mean-diameter blade section, which consists of three component drag coefficients assumed to represent profile losses, annulus-friction losses, and secondary-flow losses. The profile drag coefficient is obtained from wake-survey measurements in cascade tunnels. The remaining losses were found to be given satisfactorily, for a large number of compressors analyzed, by the empirical relations

$$C_{D,an}=0.020\ S/l \tag{20}$$

and

$$C_{D,s}=0.018\ C_L^2 \tag{21}$$

and are considered to represent annulus-friction losses and secondary-flow losses, respectively.

The increase in the effective drag coefficient due to annulus friction and secondary flow, as indicated by equations (20) and (21), represents, of course, a corresponding increase in the effective drag-lift ratio, but Howell's analysis does not indicate how this increase is to be distributed over the annulus. Survey measurements on compressors have shown, however, that the main increase in losses occurs near the ends of the blades. Thus it would seem reasonable in applying the blade-element theory to use the value of D/L obtained from cascade measurements in the middle portion of the blade and a considerably augmented value near the ends of the blades. Because of uncertainties as to how to distribute these increases and because of the breakdown near the ends of the blades of the conditions required for the blade-element theory to apply, quantitative results cannot be expected with this method of analyzing the stage efficiency. The blade-element theory may be used, however, as a qualitative guide in design until more exact methods of analysis are available.

The theoretical optimum value of $w_m=1$ for constant D/L may be altered somewhat if D/L varies with w_m. Actually D/L appears to decrease slightly as w_m is decreased. Thus the optimum value of w_m may be somewhat less than 1. In any case, as is shown in figure 5, the decrease in blade-element efficiency is small for moderate deviations from the optimum value of w_m. Also for any deviations from a symmetrical velocity diagram, the losses are less when the deviation on either blade row is toward smaller values of w_m because the ideal pressure rise, which is the weighting factor for calculating (incompressible) stage efficiency, is then less on the less efficient blade row. The blade-element theory also indicates that the significant factor is the drag-lift

ratio and not merely the drag. Thus a decrease in the lift coefficient, such as might be produced by an excessively high solidity, reduces the efficiency the same as an increase in drag coefficient. Because the stage efficiency depends also to a considerable extent on the losses associated with secondary flow not considered in the blade-element theory, the need for research on the details of three-dimensional flow is indicated.

COMPRESSOR SIZE

The blade-element theory shows for subsonic designs the possibility of decreasing both the diameter and the length of a compressor for a given air flow and pressure ratio by careful consideration of the velocity distribution. A superficial consideration of figures 7 and 11 would suggest that for constant relative Mach number any effort to reduce the diameter by decreasing w_m in order to increase the specific mass flow would necessarily decrease the pressure ratio per stage and thereby increase the compressor length. This argument, however, considers only a single blade element and neglects the actual limitations that occur in a multistage compressor. First, once the rotor speed is fixed for any reason, the pressure ratio across a blade element can be increased by decreasing the value of w_m to the point where the limiting Mach number is reached, as shown for the case of a symmetrical diagram by figure 8. Secondly, the specific mass flow limits the mass flow of the compressor only at the inlet to the compressor. Because the inlet stage tends to limit both the mass flow and the rotor speed of a compressor, the consideration of velocity distribution in the inlet stage is particularly important.

A low hub-to-tip-diameter ratio at the inlet is desirable for high mass flow through a given diameter. For the conventional type of axial-flow stage, ratios much below 0.5 appear impractical because of the impossibility of maintaining favorable velocity diagrams at all radii, but lower values might be effectively used in a very high-solidity stage with considerable hub taper. The design would then approach that typical of "mixed-flow" compressors with appreciable pressure rise along the hub arising from centrifugal action; the terms involving ω in equation (4) would no longer be negligible. The next section is concerned only with the more conventional type of design.

Velocity distribution in inlet stage.—The method of design based on free-vortex flow is widely used because of the simplicity and the relatively high accuracy with which the flow can be calculated. The velocity diagrams for a free-vortex design for high specific mass flow with a hub-to-tip-diameter ratio of 0.55 are shown in figure 12 (a). For simplicity, the effect of passage taper is neglected. The maximum pressure ratio compatible with this type of design was obtained by making the maximum Mach number the same (0.7) on the rotor and stator blades. The maximum Mach number occurs at the tip on the rotor blades and at the hub on the stator blades.

The blade-element theory shows that this type of design has several disadvantages. The velocity diagram is unsymmetrical at all but one radius and the inlet Mach number

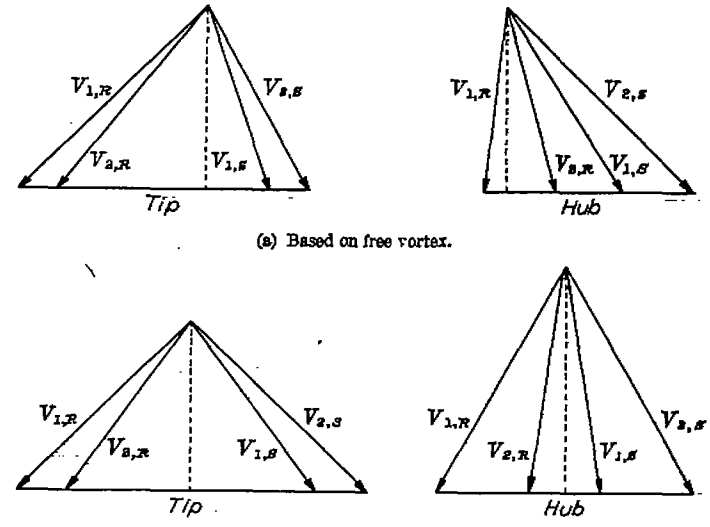

(a) Based on free vortex.

(b) Based on symmetrical velocity diagram and constant total enthalpy along radius.

FIGURE 12.—Velocity diagrams for first rotor row of multistage compressor for high specific mass flow with hub-to-tip-diameter ratio of 0.55 and maximum product of lift coefficient and solidity $(C_L\sigma)_{max}$ of 0.77.

for most of the blade length is much below the limiting value. The result is a rather low pressure ratio per stage and, at the hub, a relative velocity at the outlet of the rotor actually greater than at the inlet. It has been suggested that difficulties might arise at the hub with blades designed for such a velocity diagram because the required blade curvature in the direction of rotation at the rotor outlet would tend to start the flow in the opposite direction from that desired. The cause for this uncertainty of flow direction and the possibility of backflow can be eliminated by making the velocity diagram more symmetrical at the hub, but the pressure ratio of the stage is further reduced by this adjustment inasmuch as the limiting Mach number is then no longer attained on both the rotor and stator blades.

The use of a symmetrical velocity diagram with constant total enthalpy at all radii (fig. 12(b)) eliminates these disadvantages. The same Mach number and $C_L\sigma$ limitations are used as for the free-vortex design. The principal difference is that the inlet Mach number is very nearly constant for all blade elements of both rotor and stator blades. The inlet Mach number at the hub is actually slightly higher than at the tip because of the increase in axial velocity toward the hub required for this type of rotation to maintain radial equilibrium. The specific mass flow is also somewhat higher for the symmetrical velocity diagram than for a free vortex because of the increase in axial velocity toward the hub. A comparison of the weighted average specific mass flow and the pressure ratio for the two types of velocity distribution with the same maximum inlet Mach number for each is shown in the following table:

	$w\sqrt{\theta}/\delta A$	p_2/p_1	$\frac{\Delta p_{vortex}}{\Delta p_{symmetrical\ diagram}}$
Symmetrical diagram	37.4	1.136	
Free vortex, same $(C_L\sigma)_h$	35.1	1.087	0.64
Free vortex, same $(-\Delta w)_h$	35.2	1.091	.67

Limitations on turning based on both $C_L\sigma$ and on $-\Delta w$ are shown. The limitations are conservative but are the same for both types of design and should therefore give the relative, but not necessarily the maximum, performance for the two designs. Not only is the pressure ratio for the inlet stage higher for the symmetrical diagram than for the vortex but also the pressure ratio obtainable in the succeeding stages is higher because of the higher rotor speed permitted for the symmetrical-design diagram (12-percent higher rotor speed for this example).

A disadvantage of the design based on symmetrical velocity diagram and constant total enthalpy along the radius is that the axial velocity may become very low or the solution become impossible (imaginary velocity) near the tip, especially after the rotor, for low mass flow. The decrease in axial velocity across the rotor blades at the tip is not shown in the velocity diagram. The variation in axial velocity from hub to tip is useful in producing a more uniform inlet Mach number but, if too large, results in flow separation along the casing. The magnitude of the radial variation in axial velocity for the symmetrical-diagram design is a function of w_m at some particular radius, such as the hub, and increases with increasing values of w_m. The axial velocity at the casing may become 0 if the value of w_m at the hub is made too large. The design based on a symmetrical velocity diagram and constant total enthalpy along the radius is therefore suitable only for designs with high specific mass flow. A velocity distribution somewhere between a free-vortex design and a symmetrical velocity diagram at all radii would probably be preferable for designs of lower specific mass flow than that considered in the example of figure 12 (b). Small variations in the total enthalpy along the radius may also be useful in obtaining a favorable radial variation in the velocity components. The determination of the theoretical optimum distribution of velocity and enthalpy is very complex because of the infinite number of possible variations, but a good approximation to an optimum design for given conditions is possible with the aid of the blade-element theory.

Axial variations through compressor.—The blade-element theory is also very useful in the analysis of the effect of different variations of axial velocity from stage to stage. The speed of the rotor is usually determined by the Mach number limitation on the first row of rotor blades. For maximum pressure ratio per stage, an increase in the blade velocity U in the later stages would be desirable. In the usual designs, the angular velocity of all the rotor blades is the same because they are mounted on the same shaft. The blade-element velocity U, however, can be increased by increasing the radial distance from the axis. The increase in the tip diameter, however, increases the over-all diameter of the compressor for a given specific mass flow at the compressor inlet. If a larger over-all diameter is to be used, the use of the larger diameter also at the inlet would appear desirable in order to allow a higher hub-to-tip-diameter ratio with a given mass flow and thus to obtain higher pressure ratios over the first few stages. The increase in the tip diameter in the later stages therefore is of dubious value.

The increase in hub diameter from stage to stage, however, produces a higher pressure ratio per stage both by increasing the blade-element velocity at the hub U_h and by maintaining the inlet Mach number near the limiting value by an increase in axial velocity (fig. 8). The maximum pressure ratio with a constant casing diameter is obtained by increasing the hub diameter from stage to stage in such a manner as to obtain the limiting inlet Mach number on each stage. Because the velocity of sound increases, the axial velocity at the casing must be increased to maintain the same inlet Mach number. For pressure ratios of 5 or more, this procedure leads to very short blades and high ratios of hub-to-tip diameter in the last stages. The tip-clearance losses are increased unless the absolute clearances are reduced because of the greater relative clearance for the short blades. The annulus losses may also be a larger percentage of the energy input because of higher ratio of passive, or annulus, area to active, or blade, area (reference 12). The use of small blade chords will reduce this ratio of passive to active area as well as reduce the length of the compressor, but the adverse effect of reducing the Reynolds number must be considered (reference 12). Because of the relatively high density and velocity in the last stages, however, the chords can be made considerably smaller than in the inlet stages and the same Reynolds number maintained. The diffuser requires more careful attention with high axial velocities at the compressor outlet but the diffuser losses become less important as the over-all pressure ratio is increased. The use of boundary-layer control, even for high outlet velocities, should make efficient diffusion possible in a very short diffuser (reference 13). The required suction could easily be provided. For example, the boundary-layer air removed might be used for cooling some portion of the turbine where the pressure is lower than that in the diffuser.

The high losses reported by Eckert (reference 12) for high hub-to-tip-diameter ratios in single-stage blowers appear to be less serious in multistage compressors. The hub-to-tip-diameter ratio is quite high in the last few stages of the NACA eight-stage axial-flow compressor (0.93 in the last stage). (See reference 2.) Although no information is available on the efficiency of the last stages, the over-all efficiency (references 1, 2, and 14) is much higher than would be expected if the efficiency dropped as drastically as indicated by Eckert.

FLEXIBILITY AND RANGE

Very little has yet been done on the investigation of the effect of design variables on the range and the flexibility of axial-flow compressors. An unpublished British report made a theoretical analysis based on cascade data of several types of design, but the differences in range for practical designs were not particularly remarkable. The problem of range and flexibility is considered from an entirely different point of view in reference 1, where the possible extension of the useful range by the use of adjustable stator-blade settings is investigated. Improvements in the efficiency at other than design speed and a considerable extension of the flow range at any given speed were found to be possible by the adjustment of the stator-blade angles alone. An improvement of about 0.08 in efficiency over the design setting for one of the

blade resettings at approximately half the design speed was obtained. A shift of the peak-efficiency flow by 20 to 30 percent was possible over the entire speed range by the use of different stator-blade-angle settings. The extension in the flow range was particularly striking at a compressor Mach number of 0.8 because of the very narrow range at this speed with any one blade setting. Approximately a sevenfold increase in the flow range was obtained at this compressor speed by the use of different stator-blade settings.

The success of this method in extending the useful range of axial-flow compressors has warranted the development of a more rapid method for computing blade resettings than that presented in reference 1. Figures 3, 4, and 6 provide the basis for such a method, as is illustrated by the example in appendix B.

SUMMARY OF ANALYSIS

A blade-element theory developed for analyzing the effect of basic design variables on axial-flow-compressor performance may be summarized as follows:

The one-dimensional compressible-flow theory shows that the effect of polytropic efficiency on some of the flow relations across a row of blades is of the same order of magnitude as the effect of Mach number. Flow calculations based on isentropic compressible flow may therefore be appreciably in error. For substantial improvement in compressor efficiency, research should be directed toward a reduction in blade-element drag-lift ratio and toward a better understanding of secondary-flow phenomena.

The relative Mach number is shown to be a dominant factor in determining the pressure ratio and considerable increase in pressure ratio over that for conventional designs can be obtained by producing a velocity distribution that gives relative inlet Mach numbers close to the limiting Mach number on all blade elements. With a given inlet Mach number, the pressure ratio obtainable across a blade row increases and the specific mass flow decreases as the ratio of mean whirl velocity to axial velocity increases for the high-efficiency range of this velocity ratio (values near 1).

For compressor designs with a definite Mach number limitation, the velocity distribution in the inlet stage is particularly important because the inlet stage limits both the mass flow and the rotor speed of the compressor and thereby limits the pressure ratio of later stages as well as the inlet stage. By the use of inlet guide vanes designed to produce a radial variation of axial velocity at the inlet to the first rotor, a substantial increase in stage pressure ratio and a slight increase in the specific mass flow over designs based on free vortex with the same Mach number and turning limitations are shown to be possible. In the succeeding stages, the maximum pressure ratio per stage without an increase in compressor diameter is obtainable by increasing the hub diameter to obtain the maximum axial velocity compatible with the Mach number limitation.

The use of adjustable stator blades is an effective method of extending the high-efficiency range of axial-flow compressors. A graphical method developed for one-dimensional analysis is very useful in determining the blade-angle settings for different operating conditions.

FLIGHT PROPULSION RESEARCH LABORATORY,
NATIONAL ADVISORY COMMITTEE FOR AERONAUTICS,
CLEVELAND, OHIO, *November 26, 1947.*

APPENDIX A

DERIVATION OF EQUATIONS

When an equation is the same as in the body of the text the equation number is the same.

Adiabatic and polytropic efficiencies.—For different ideal reversible processes, such as adiabatic, isothermal, and polytropic, the densities are different functions of the pressure and therefore by equation (7) the efficiencies obtained are different. Because most actual compression processes are approximately adiabatic, the efficiency based on a reversible adiabatic process as the ideal process has been widely used. The polytropic efficiency is also useful because it is equal to the efficiency of the individual small stages of an adiabatic compression when the efficiency of these small stages is constant throughout. For this reason, it is often referred to as "small-stage" efficiency. For constant specific heat, the density is given by

$$\rho=\rho_1\left(\frac{p}{p_1}\right)^{1/\gamma} \tag{22}$$

for the reversible adiabatic process and by

$$\rho=\rho_1\left(\frac{p}{p_1}\right)^{1/n} \tag{23}$$

for the polytropic process. The polytropic exponent n for the ideal process is chosen to give the same density and temperature at the final pressure p_2 as for the actual process. The substitution of these expressions in equation (7) and the use of the perfect gas law gives the following values for the adiabatic and polytropic efficiencies:

$$\eta_{ad}=\frac{Rt_1\dfrac{\gamma}{\gamma-1}\left[\left(\dfrac{p_2}{p_1}\right)^{\frac{\gamma-1}{\gamma}}-1\right]}{\Delta h} \tag{24}$$

$$\eta_p=\frac{Rt_1\dfrac{n}{n-1}\left[\left(\dfrac{p_2}{p_1}\right)^{\frac{n-1}{n}}-1\right]}{\Delta h} \tag{25}$$

The thermodynamic relations

$$\Delta h=Jc_p(t_2-t_1)=R\frac{\gamma}{\gamma-1}t_1\left(\frac{t_2}{t_1}-1\right) \tag{26}$$

and

$$\left(\frac{p_2}{p_1}\right)^{\frac{n-1}{n}}=\frac{t_2}{t_1} \tag{27}$$

when substituted in equations (24) and (25) give

$$\eta_{ad}=\frac{\left(\dfrac{p_2}{p_1}\right)^{\frac{\gamma-1}{\gamma}}-1}{\dfrac{t_2}{t_1}-1} \tag{28}$$

or

$$\eta_{ad}=\frac{\left(\dfrac{p_2}{p_1}\right)^{\frac{\gamma-1}{\gamma}}-1}{\left(\dfrac{p_2}{p_1}\right)^{\frac{n-1}{n}}-1}$$

and

$$\eta_p=\frac{n/(n-1)}{\gamma/(\gamma-1)} \tag{29}$$

Therefore

$$\eta_{ad}=\frac{\left(\dfrac{p_2}{p_1}\right)^{\frac{\gamma-1}{\gamma}}-1}{\left(\dfrac{p_2}{p_1}\right)^{\frac{\gamma-1}{\gamma\eta_p}}-1} \tag{8}$$

By the use of L'Hospital's rule, the limiting value of η_{ad} as p_2/p_1 approaches 1 can readily be shown to be equal to η_p.

If equation (29) is solved for n, the polytropic exponent is given as a function of the polytropic efficiency

$$n=\frac{\eta_p}{\eta_p-\dfrac{\gamma-1}{\gamma}} \tag{9}$$

Although the derivation has been made in terms of static pressures, temperatures, and enthalpies, each of the equations in this derivation can readily be shown to apply when the static values are replaced by the corresponding total values. For a given process, the efficiencies and the polytropic exponent based on total and static values will differ, but, as was shown by the example in the section General Efficiency Relations, when these efficiencies are used to represent the over-all performance of a compressor the differences between the corresponding efficiencies based on total and static values is usually quite small.

Relation between total and static efficiencies.—The adiabatic efficiency based on total pressures and temperatures can readily be expressed in terms of the adiabatic efficiency based on static values by substituting in the equation defining the total efficiency

$$\eta_{ad,T}=\frac{\left(\dfrac{P_2}{P_1}\right)^{\frac{\gamma-1}{\gamma}}-1}{\dfrac{T_2}{T_1}-1}$$

the relations between total and static pressures and temperatures

$$\frac{T}{t}=\left(\frac{P}{p}\right)^{\frac{\gamma-1}{\gamma}}=1+\frac{\gamma-1}{2}M^2$$

where the values are with respect to a stationary reference frame. Thus,

$$\eta_{ad,T}=\frac{C\left(\dfrac{p_2}{p_1}\right)^{\frac{\gamma-1}{\gamma}}-1}{C\left(\dfrac{t_2}{t_1}\right)-1} \tag{30}$$

where

$$C=\frac{1+\dfrac{\gamma-1}{2}M_2^2}{1+\dfrac{\gamma-1}{2}M_1^2}$$

When $M_1=M_2$, then $C=1$, and equation (30) becomes the same as the relation for the static efficiency

$$\eta_{ad,st}=\frac{\left(\frac{p_2}{p_1}\right)^{\frac{\gamma-1}{\gamma}}-1}{\frac{t_2}{t_1}-1} \tag{31}$$

An explicit relation for the total efficiency in terms of the static efficiency and the static-pressure ratio can be obtained by eliminating the temperature ratio in equation (30) by use of equation (31). The result of this elimination is

$$\eta_{ad,T}=\eta_{ad,st}\frac{C\left(\frac{p_2}{p_1}\right)^{\frac{\gamma-1}{\gamma}}-1}{\left[C\left(\frac{p_2}{p_1}\right)^{\frac{\gamma-1}{\gamma}}-1\right]+(1-C)(1-\eta_{ad,st})}$$

or expressed in terms of total-pressure ratio

$$\eta_{ad\ T}=\eta_{ad,st}\frac{\left(\frac{P_2}{P_1}\right)^{\frac{\gamma-1}{\gamma}}-1}{\left(\frac{P_2}{P_1}\right)^{\frac{\gamma-1}{\gamma}}-1+(1-C)(1-\eta_{ad,st})}$$

By a similar derivation,

$$\eta_{p,T}=\eta_{p,st}\frac{\log\left(\frac{P_2}{P_1}\right)^{\frac{\gamma-1}{\gamma}}}{\log\left(\frac{P_2}{P_1}\right)^{\frac{\gamma-1}{\gamma}}-(1-\eta_{p,st})\log C}$$

Blade-element efficiency.—A blade-element efficiency for incompressible flow based on the power input to the air by the rotor is suitable if applied to an entire stage, as in reference 2, but is unsuitable for considering the performance of a single blade row. For flow across a single blade row with no change in radius and with the blade row as reference frame,

$$\Delta h=\frac{1}{g}\left(\frac{V_1^2}{2}-\frac{V_2^2}{2}\right) \tag{32}$$

and the general expression for efficiency based on static states (equation (7)) becomes, for the case of incompressible flow considered herein,

$$\eta_{st,i}=\frac{\Delta p}{\frac{\rho V_1^2}{2}-\frac{\rho V_2^2}{2}} \tag{33}$$

which is the usual simplified expression for diffuser efficiency in which velocity variations across the passage are neglected (reference 15).

For constant axial velocity, the following relations can readily be obtained from momentum considerations and figures 1 and 13:

$$\Delta p=\frac{F_a}{S}=\frac{1}{S}(L\sin\beta_m-D\cos\beta_m)$$

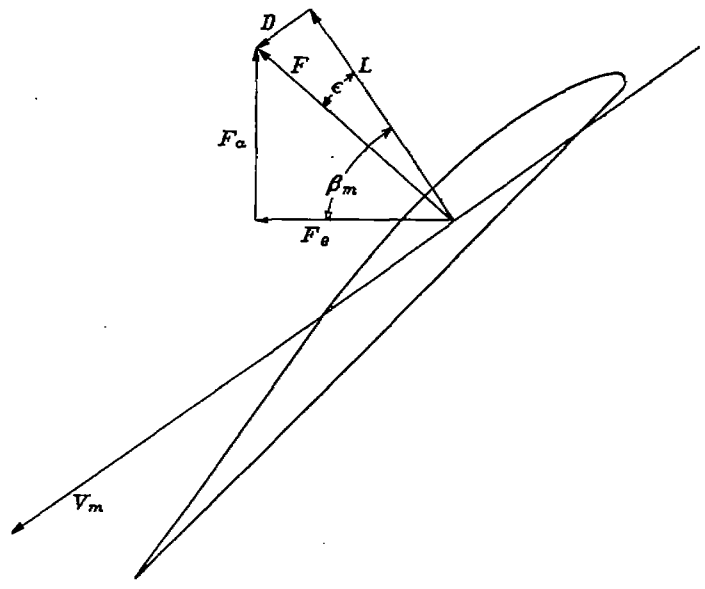

FIGURE 13.—Vector diagram of forces on blade element.

$$=\frac{L\sin\beta_m}{S}\left(1-\frac{D}{L}\cot\beta_m\right) \tag{34}$$

and

$$L=\frac{F_\theta-D\sin\beta_m}{\cos\beta_m}$$

$$=\frac{F_\theta}{\cos\beta_m}-L\frac{D}{L}\tan\beta_m$$

or if this equation is solved for L

$$L=\frac{F_\theta}{\cos\beta_m[1+(D/L)\tan\beta_m]}$$

$$=\frac{\rho V_a^2 S(\tan\beta_1-\tan\beta_2)}{\cos\beta_m[1+(D/L)\tan\beta_m]} \tag{35}$$

If this lift is substituted in equation (34),

$$\Delta p=\frac{\rho V_a^2\tan\beta_m(\tan\beta_1-\tan\beta_2)[1-(D/L)\cot\beta_m]}{1+(D/L)\tan\beta_m}$$

$$=\frac{\rho V_a^2 w_m(-\Delta w)\left(1-\frac{1}{w_m}\frac{D}{L}\right)}{1+w_m(D/L)} \tag{36}$$

also

$$\frac{\rho V_1^2}{2}-\frac{\rho V_2^2}{2}=\frac{\rho}{2}(V_{w,1}^2-V_{w,2}^2)$$

$$=\rho V_a^2 w_m(-\Delta w) \tag{37}$$

By the substitution of equations (36) and (37) in equation (33), the blade-element efficiency based on static-pressure rise and incompressible flow is finally obtained as

$$\eta_{st,i}=\frac{1-\frac{1}{w_m}\frac{D}{L}}{1+w_m(D/L)} \tag{10}$$

The blade-element efficiency can also be expressed in terms of the "gliding angle" ϵ (fig. 13), which is defined by

$$\tan\epsilon=D/L \tag{38}$$

The profile efficiency is

$$\eta_{st,t}=\frac{\tan(\beta_m-\epsilon)}{\tan\beta_m}$$

or

$$=\frac{\tan(90°-\beta_m)}{\tan(90°-\beta_m+\epsilon)} \tag{11}$$

which is the same as the expression for the profile efficiency of a propeller.

Pressure ratios.—The pressure ratio across a row of blades for constant axial velocity and no radial flow can be expressed in terms of w_m, $-\Delta w$, and M by use of equation (12) and figure 1(b)

$$\frac{p_2}{p_1}=\left(1+\frac{\gamma-1}{2}M_1^2\frac{V_1^2-V_2^2}{V_1^2}\right)^{\frac{\gamma\eta_p}{\gamma-1}}$$

$$=\left(1+\frac{\gamma-1}{2}M_1^2\frac{V_a^2}{V_1^2}\frac{V_{w,1}^2-V_{w,2}^2}{V_a^2}\right)^{\frac{\gamma\eta_p}{\gamma-1}}$$

$$=\left[1+(\gamma-1)M_1^2\frac{V_a^2}{V_1^2}\frac{V_{w,1}+V_{w,2}}{2V_a}\frac{V_{w,1}-V_{w,2}}{V_a}\right]^{\frac{\gamma\eta_p}{\gamma-1}}$$

$$=\left\{1+(\gamma-1)M_1^2\frac{w_m(-\Delta w)}{1+\left[w_m+\frac{(-\Delta w)}{2}\right]^2}\right\}^{\frac{\gamma\eta_p}{\gamma-1}} \tag{15}$$

Specific mass flow.—The mass flow through a unit cross-sectional area in terms of a stationary reference frame is

$$\frac{W}{A}=g\rho V_a$$

$$=g\rho_T a_T\frac{\rho}{\rho_T}\frac{a}{a_T}\frac{V_S}{a}\cos\beta_S$$

$$=g\rho_T a_T\frac{M_S\cos\beta_S}{\left(1+\frac{\gamma-1}{2}M_S^2\right)^{\frac{\gamma+1}{2(\gamma-1)}}} \tag{17}$$

$$=\frac{P\sqrt{\gamma g}}{\sqrt{RT}}\frac{M_S\cos\beta_S}{\left(+\frac{\gamma-1}{2}M_S^2\right)^{\frac{\gamma+1}{2(\gamma-1)}}}$$

$$=\frac{P}{p_0}\sqrt{\frac{t_0}{T}}\frac{p_0\sqrt{\gamma g}}{\sqrt{Rt_0}}\frac{M_S\cos\beta_S}{\left(1+\frac{\gamma-1}{2}M_S^2\right)^{\frac{\gamma+1}{2(\gamma-1)}}}$$

For $\gamma=1.4$ and $R=53.345$ (dry air)

$$\frac{W}{A}=\frac{\delta}{\sqrt{\theta}}\frac{2116.2\sqrt{1.4\times32.174}}{\sqrt{53.345\times518.6}}\frac{M_S\cos\beta_S}{(1+0.2M_S^2)^3}$$

Hence

$$\frac{W\sqrt{\theta}}{\delta A}=\frac{85.4M_S\cos\beta_S}{(1+0.2M_S^2)^3} \tag{18}$$

In order to express this result in terms of the relative Mach number and the velocity diagram parameters for a symmetrical velocity diagram, it must be remembered that the quantities in equation (18) are for absolute coordinates at the inlet to the rotor (station 1). With the aid of figure 9, the following substitutions may be made in equation (18):

$$\frac{W\sqrt{\theta}}{\delta A}=\frac{85.4\frac{V_a}{V_{1,R}}\frac{V_{1,R}}{a_1}}{\left[1+0.2\left(\frac{V_{1,R}}{a_1}\right)^2\left(\frac{V_{1,S}}{V_{1,R}}\right)^2\right]^3}$$

$$=\frac{85.4\frac{V_a}{V_{1,R}}M_{1,R}}{\left[1+0.2M_{1,R}^2\left(\frac{V_{2,R}}{V_{1,R}}\right)^2\right]^3}$$

$$=\frac{85.4M_{1,R}}{\left\{1+0.2M_{1,R}^2\frac{1+\left[w_m-\frac{(-\Delta w)}{2}\right]^2}{1+\left[w_m+\frac{(-\Delta w)}{2}\right]^2}\right\}^3\sqrt{1+\left[w_m+\frac{(-\Delta w)}{2}\right]^2}}$$

The value of $-\Delta w$ is given in terms of $C_L\sigma$ by equation (16).

APPENDIX B

EXAMPLE OF USE OF CHARTS FOR COMPUTATION OF STATOR-BLADE RESETTING

The method of computing the stator-blade resetting for different operating conditions given in reference 1 involves considerable labor in the trial-and-error solution of the velocity-ratio equation (equation (19) of reference 1). Enlarged working charts similar to figures 3, 4, and 6 greatly facilitate the computation of stator-blade resetting, as is illustrated by the following example:

The computations are made for a typical stage of the NACA eight-stage axial-flow compressor for an air flow and a speed appreciably below the design values. The conditions at the inlet to the stage are determined by the flow from the previous stage and, for the purpose of this example, are assumed to be known. The stage is here taken as a row of stator blades followed by a row of rotor blades. The station designations are: 1, at inlet to stator blades; 2, between stator and rotor blades; and 3, at outlet from rotor blades. Quantities that are a function of the radius are taken at the mean radius unless otherwise specified. The following geometric characteristics of the stage are given:

$$A_1/A_2=1.118$$
$$A_2/A_3=1.127$$
$$\psi_{stator}=45.3°$$
$$\psi_{rotor}=43.1° \text{ (design values)}$$
$$\alpha_0=-5.6° \text{ (for blades used)}$$
$$\sigma_{stator}=0.9961$$
$$\sigma_{rotor}=1.0156$$

and

$$r_2/r_{2,t}=0.9004$$

The given inlet conditions and rotor speed are

$$\beta_1=65.3°$$
$$V_1/a_1=0.492$$
$$U_t/a_1=0.708$$

It is proposed to reset the stator blades to make the maximum lift coefficient at the mean radius, which may occur on either the stator or the rotor blades, equal to a prescribed value of 0.8. The adjustment of the stator-blade angle to give a prescribed lift coefficient on the stator blades may be accomplished very simply by the use of figure 6 and the empirical relation from reference 1 (equation (17)):

$$\beta_2=(1-K)\beta_1+K\psi_{stator}+K\alpha_0$$

but the lift coefficient on the rotor blades also must be checked in order to determine whether the prescribed maximum is exceeded. If the prescribed maximum lift coefficient is exceeded on the rotor blades, as it is in this example, the lift coefficient must be determined with different stator-blade settings until the prescribed maximum lift coefficient is obtained on the rotor blades. The calculation of the stator-blade setting for a lift coefficient of 0.8 on the stators is first made and the resulting lift coefficient on the rotor blades determined. The calculation for the final trial solution for a lift coefficient of 0.8 on the rotor blades is then presented.

For simplicity, the value of K is assumed to be 0.9 throughout. Somewhat more accurate results could be obtained by estimating the value of K from the values presented in reference 16. A polytropic efficiency η_p of 0.9 is also assumed. The turning angle $\beta_1-\beta_2$ is found from figure 6 for

$$C_L\sigma=0.8\times0.9961=0.797$$

and, for β_1 equal to 65.3°, is 11.5°.

Therefore

$$\beta_2=53.8°$$

and from the relation

$$\beta_2=0.1\beta_1+0.9\,\psi_{stator}-0.9\times5.6$$

the value of ψ_{stator} is determined as 58.1°.

The value of C_L for the rotor blades for this strator-blade setting requires the calculation of the flow across the stator. The flow-area ratio is

$$\frac{f_1}{f_2}=\frac{A_1\cos\beta_1}{A_2\cos\beta_2}=1.118\,\frac{\cos 65.3°}{\cos 53.8°}=0.791$$

By the use of figures 3(c) and 4(c) with $df_1/df_2=0.791$ and $M_1=0.492$, the following ratios are obtained: $V_2/V_1=0.754$, $t_2/t_1=1.021$, and $a_2/a_1=1.010$. The flow conditions of the air leaving the stator row may now be obtained from the following relations:

$$\frac{V_2}{a_2}=\frac{V_2}{V_1}\frac{V_1}{a_1}\frac{a_1}{a_2}=\frac{0.754\times0.492}{1.010}=0.367$$

$$\frac{V_{a,2}}{a_2}=\frac{V_2\cos\beta_2}{a_2}=0.367\cos 53.8°=0.217$$

$$\frac{V_{w,2}}{a_2}=\frac{V_2}{a_2}\sin\beta_2=0.367\sin 53.8°=0.296$$

$$\frac{U_2}{a_2}=\frac{U_{2,t}}{a_1}\frac{r_2}{r_{2,t}}\frac{a_1}{a_2}=\frac{0.708\times0.9004}{1.010}=0.631$$

The whirl component of the Mach number relative to the rotor is then given by

$$\frac{V_{w,2,R}}{a_2}=\frac{U_2}{a_2}-\frac{V_{w,2,S}}{a_2}=0.631-0.296=0.335$$

The air velocity and the air angle relative to the rotor are then obtained from the relations (in which the subscript R has been dropped)

$$\tan\beta_2=\frac{V_{w,2}/a_2}{V_{a,2}/a_2}=\frac{0.335}{0.217}=1.544$$

$$\beta_2=57.1°$$

$$\frac{V_2}{a_2}=\frac{V_{w,2}/a_2}{\sin\beta_2}=\frac{0.335}{0.840}=3.999$$

The leaving-air angle may now be obtained from the relation

$$\begin{aligned}\beta_3&=(1-K)\beta_2+K\psi_{\text{rotor}}+K\alpha_0\\&=(1-0.9)57.1°+0.9(43.1°)+0.9(-5.6°)\\&=39.5°\end{aligned}$$

The flow-area ratio across the rotor row is now obtained from

$$\frac{f_2}{f_3}=\frac{A_2}{A_3}\frac{\cos\beta_2}{\cos\beta_3}=1.127\frac{\cos 57.1°}{\cos 39.5°}=0.792$$

Using figures 3(c) and 4(c) again with $df_1/df_2=0.792$ and $M_1=0.399$ (with the obvious changes in subscripts) gives

$$\frac{V_3}{V_2}=0.770$$

$$\frac{t_3}{t_2}=1.013$$

$$\frac{a_3}{a_2}=1.006$$

and the conditions at the exit of the rotor row are

$$\frac{V_3}{a_3}=\frac{V_3}{V_2}\frac{V_2}{a_2}\frac{a_2}{a_3}=\frac{0.770\times 0.399}{1.006}=0.305$$

$$\frac{V_{a,3}}{a_3}=\frac{V_3}{a_3}\cos\beta_3=0.305\cos 39.5°=0.235$$

$$\frac{V_{w,3}}{a_3}=\frac{V_3}{a_3}\sin\beta_3=0.305\sin 39.5°=0.194$$

The turning angle for the rotor row is $\beta_2-\beta_3=57.1°-39.5°=17.6°$. Now by use of figure 6, $C_L\sigma=0.93$, which gives a lift coefficient on the rotor

$$C_L=\frac{0.93}{1.0156}=0.92$$

This lift coefficient exceeds the maximum prescribed value of 0.8. The lift coefficient on the rotor row therefore must be lowered by increasing the stator-blade angles. The stator lift coefficient will also be unavoidably reduced.

After several trials, a value of $\psi_{\text{stator}}=60°$ was found to give approximately the maximum prescribed lift coefficient of 0.8 on the rotor blades. The lift coefficient on the stator blade for this setting was 0.69.

REFERENCES

1. Sinnette, John T., Jr., and Voss, William J: Extension of Useful Operating Range of Axial-Flow Compressors by Use of Adjustable Stator Blades. NACA Rep. No. 915, 1948.
2. Sinnette, John T., Jr., Schey, Oscar W., and King, J. Austin: Performance of NACA Eight-Stage Axial-Flow Compressor Designed on the Basis of Airfoil Theory. NACA Rep. No 758, 1943.
3. Sörensen, E.: Constant-Pressure Blowers. NACA TM No. 927, 1940.
4. Betz, A., and Flügge-Lotz, I.: Design of Centrifugal Impeller Blades. NACA TM No. 902, 1939.
5. Sorg, K. W.: Supersonic Flow in Turbines and Compressors. R. A. S. Jour., vol. XLVI, no. 375, March 1942, pp. 64–85.
6. Van Driest, E. R.: Steady Turbulent-Flow Equations of Continuity, Momentum, and Energy for Finite Systems. Jour. Appl. Mech., vol. 13, no. 3, Sept. 1946, pp. A231–A238.
7. Moss, Sanford A., Smith, Chester W., and Foote, William R.: Energy Transfer between a Fluid and a Rotor for Pump and Turbine Machinery. A. S. M. E. Trans., vol. 64, no. 6, Aug. 1942, pp. 567–597.
8. Keller, Curt: The Theory and Performance of Axial-Flow Fans. (Adapted for the use of fan designers by Lionel S. Marks and John R. Weske.) McGraw-Hill Book Co., Inc., 1937.
9. Mutterperl, William: High-Altitude Cooling. VI—Axial-Flow Fans and Cooling Power. NACA ARR No. L4I11e, 1944.
10. Bell, E. Barton: Test of a Single-Stage Axial-Flow Fan. NACA Rep. No. 729, 1941.
11. Howell, A. R.: Fluid Dynamics of Axial Compressors. Inst. Mech. Eng. Proc. (British), vol. 153 (War Emergency Issue No. 1), 1945, pp. 441–452.
12. Eckert, B.: The Influence of Physical Dimensions (Such as Hub: Tip, Ratio, Clearance, Blade Shape) and Flow Conditions (Such as Reynolds Number and Mach Number) on Compressor Characteristics. Part A—Summary of the Results of Research on Axial Flow Compressors at the Stuttgart Research Institute for Automobiles and Engines. W. A. C. Eng. Trans. No. 22, Wright Aero. Corp. (Vol. 3 of series of articles on compressor and fan design, written by German engineers, coordinated by Code 338, BuShips, Navy Dept. (Washington, D.C.), May 1946.)
13. Ackeret, J.: Removing Boundary Layer by Suction. NACA TM No. 395, 1927.
14. King, J. Austin, and Regan, Owen W.: Performance of NACA Eight-Stage Axial-Flow Compressor at Simulated Altitudes. NACA ACR No. E4L21, 1944.
15. Patterson, G. N.: Modern Diffuser Design. Aircraft Eng., vol. X, no. 115, Sept. 1938, pp. 267–273.
16. Bogdonoff, Seymour M., and Bogdonoff, Harriet E.: Blade Design Data for Axial-Flow Fans and Compressors. NACA ACR No. L5F07a, 1945.

905335—50——14